DSD Characterization and Computations of Expected Reflectivity using Data from a Two-Dimensional Video Disdrometer Deployed in Puerto Rico

by

José G. Maeso-González

A thesis submitted in partial fulfillment of the requirements for the degree of

MASTER OF SCIENCE
in
ELECTRICAL ENGINEERING

UNIVERSITY OF PUERTO RICO
MAYAGÜEZ CAMPUS
2005

Approved by:

_____	_____
Sandra L. Cruz Pol, PhD President, Graduate Committee	Date
_____	_____
José Colom Ustáriz, PhD Member, Graduate Committee	Date
_____	_____
H. Mario Ierkic, PhD Member, Graduate Committee	Date
_____	_____
Eric Harmsen, PhD Representative of Graduate Studies	Date
_____	_____
Isidoro Couvertier, PhD Chairperson of the Department	Date
_____	_____
José Mari-Mutt, PhD Director of Graduate Studies	Date

ABSTRACT

Accurate estimation of drop size distribution (DSD) for all rain rates is necessary to develop and validate rainfall retrieval algorithms. The Two-Dimensional Video Disdrometer (2DVD) presented in this research offers a new approach to measuring DSDs.

A 2DVD was deployed in Puerto Rico. An initial DSD characterization was performed to compare with previous studies. The event considered was Tropical Storm Jeanne that passed on September 15th and 16th, 2004. Preliminary results confirmed that DSDs are highly variable between coastal and mountainous regions, as suggested by Ulbrich (1999), even in a small island like this.

In addition, this work intends to improve the reliability of rain algorithms used in tropical regions, expecting to enhance rainfall rates (R) estimation. The expected radar reflectivity Z is calculated from 2DVD-measured DSDs and compared with measured Z from the National Weather Service WSR-88D radar. Different Z-R relationships for both days are obtained from these calculations.

RESUMEN

El estimado certero de la distribución de los tamaños para las gotas de lluvia, conocido en inglés como "drop size distribution" o DSD, para todas las tasas de lluvia – intensidades de precipitación (R) – es necesario para desarrollar y validar los algoritmos utilizados en los cómputos de la cantidad de precipitación. El Disdrómetro de Video de Dos Dimensiones (2DVD, por sus siglas en inglés) presentado en esta investigación ofrece un acercamiento nuevo para la medida de las distribuciones de los tamaños.

Un 2DVD fue instalado en Puerto Rico. Se realizó una caracterización inicial de las distribuciones para compararla con estudios previos. El evento considerado fue la Tormenta Tropical Jeanne que pasó por Puerto Rico el 15 y 16 de septiembre de 2004. Los resultados preliminares confirmaron que las distribuciones de los tamaños de las gotas son altamente variables entre las regiones costeras y las montañosas, como lo sugirió Ulbrich (1999), aun en una pequeña isla como ésta.

Adicionalmente, este trabajo intenta aumentar la confiabilidad de los algoritmos de precipitación usados para las regiones tropicales, esperando mejorar el cómputo de las intensidades de lluvia. El cálculo de la reflectividad Z que mediría un radar es obtenido de las distribuciones de tamaños medidas por el 2DVD y comparadas con la Z medida por el radar WSR-88D del Servicio Nacional de Meteorología local. Diferentes relaciones Z-R fueron obtenidas de estos cómputos para cada día de la tormenta.

To God, my mom, grandmother, and aunt Ana Rosa…

ACKNOWLEDGEMENTS

During my graduate studies in the University of Puerto Rico several persons and institutions collaborated directly and indirectly with my research. Without their support it would be impossible finish my work. That is why I wish to dedicate this section to recognize their support.

I want to start expressing a sincere acknowledgement to my advisor, Dr. Sandra Cruz-Pol because she gave me the opportunity to research under her guidance and supervision. I received motivation, encouragement, and support from her during all my studies, even in personal issues. With her, I learned how to better share my ideas to others, visually and written. I also want to thank the motivation and support I received from Dr. José Colom. From these two persons, I am completely grateful. They set a model of how professors can not only be academic advisors but also be a factor in life; their example influenced the decision to become a professor in the future.

Thanks to NWS local WFO personnel, Israel Matos, Bert Gordon, Wilfredo Muñoz, Marlon Carter, and especially to Rachel Gross, for providing their knowledge and help, and for making available their premises and resources for the success of this project.

Special thanks I owe to Dr. V.N. Bringi from Colorado State University (CSU) for the opportunity of researching under his supervision; his support, guidance, and transmitted knowledge accounted for the completion of my work. He provided not only his knowledge, but the utilization of his resources and the assistance of his graduate students. Thanks to Dr. V. Chandrasekar, also from CSU, for the chance of having the video disdrometer installed in Puerto Rico for more than one year and for the trust in our responsibility towards this innovative and expensive instrument. Many thanks to Dr. Michael Schönhuber from Joanneum Research from

Graz, Austria, for his disposition, recommendations and technical support regardless considerable time differences between our time zones. Thanks to Dr. Carlton Ulbrich from Clemson University for the research documentation provided and his help with equations and DSD analysis.

Thanks also to Dr. H. Mario Ierkic for serving on my committee and for his encouragement, motivation, understanding and clever ideas through my research. His judgment gave me different point of views I would have not consider otherwise.

I would like to acknowledge the Electrical and Computer Engineering Department from the University of Puerto Rico and its NASA research centers, Cloud Microwave Measurements of Atmospheric Phenomena (CLiMMATE) and the Tropical Center for Earth and Space Studies (TCESS) who provided the funding and the resources for the development of this research under Faculty Awards for Research NAG-1-02074 and University Research Center grant NCC5-518 respectively; TCESS primarily supported this work. This work also made use of CASA Engineering Research Center Shared Facilities supported by the National Science Foundation under Award Number 0313747.

I want to thank my friends for your support during graduate school. Special thanks to Margarita Baquero, Víctor Marrero, Mauricio Sánchez, José Morales, from UPRM and Miguel Gálvez from CSU. At last, but the most important I would like to thank my God and my family, for their unconditional support and love.

Table of Contents

Table List

Tables Page

Figure List

Figures Page

1 INTRODUCTION

The purpose of this thesis is to improve the calculations of expected precipitation from WSR-88D radar reflectivity measurements. This work involves two major tasks. The first one is to analyze the characteristics of the drop-size distribution for a coastal zone tropical environment. In 1999, other study performed by Ulbrich, Petitididier, and Campos, found DSDs characteristics similar to continental regions. As their study was performed in a mountainous area, they suggested DSD variations between higher areas and coastal zones. From DSD measurements, reflectivity Z and rainfall rates R are calculated using theoretical equations. With these results Z-R relationships can be derived, from which weather radars determine rainfall rates after measuring Z. Those relationships are compared with known relations used by current radars.

The next task is to compare Z measured by NEXRAD and that computed from DSDs measurements. NEXRAD data available is in 5 dBZ increments and 5 or 6 minutes time intervals; it was provided by NWS local weather forecast office. In the other hand DSD data is in one-minute time intervals, for adjustments were done to compare data from same instants. Additional adjustments in time were needed to correct for the measurements differences in altitude.

1.1 Motivation

The Collaborative Adaptive Sensing of the Atmosphere (CASA) Engineering Research Center (ERC) is aimed towards creating a new engineering paradigm in observing, detecting and predicting weather and other atmospheric phenomena [CASA web site, 2003]. One significant

part of this new effort is Quantitative Precipitation Estimation (QPE), which pursues to improve the precipitation estimates and enhance the reliability of flood prediction.

In rainfall estimation techniques, the drop size distribution (DSD) is the most fundamental component, since it governs all the microwave and rainfall integral relations. It is characterized by a high temporal and spatial variability that affects both microwave measurements from radars and ground validation. Therefore, its accurate estimation for all rain-rates is necessary in order to develop and validate rainfall retrieval algorithms [*Rincón*, 2002].

A Joss-Waldvogel disdrometer is an electromechanical device that measures drop size by sensing the impact of drops falling on a Styrofoam sensor head [*Joss*, 1967]. For this mode of operation they are also known as impact or momentum disdrometers. Average drop size distributions obtained with these more traditional disdrometers have shown similar shape as DSDs calculated from information obtained from microwave links [*Rincón*, 2001]. However, the results also indicated significant differences in the amount of drops detected. Further disagreement between the gauges and the disdrometers may imply that the disdrometers are undersampling raindrops. Several other rainfall events that have been analyzed have shown similar results. Therefore more measurements have been suggested to draw final conclusions [*Ulbrich*, 2001].

The Two-Dimensional Video Disdrometer (2DVD) offers a new approach to measuring DSDs [*Kruger* and *Krajewski*, 2001]. Under low-wind conditions it provides accurate and detailed information about drop size, terminal velocity, and drop shape, outside a controlled laboratory environment. This capability was not previously available to the atmospheric scientists. After being deployed in several areas around the world, the 2DVD was deployed in Puerto Rico, in order to acquire new information on tropical DSDs. In past studies, reflectivities

derived from DSDs have shown good relation with radar reflectivities, but not enough data to achieve statistical significance has been obtained, especially in tropical climates. Our goal is to use this instrument to characterize DSD in Puerto Rico's tropical convective environment. Impact disdrometers has been used before in Puerto Rico by Ulbrich and others, but no characterization of DSDs has been performed. Other disdrometers have been used as well, to calibrate other equipments such as radars.

Regarding single polarization radars, it has been shown that huge overestimation of the rain-rate has occurred, especially in storm events [*Vázquez*, 2001]. Puerto Rico is serviced by a WSR-88D radar, also known as NEXRAD, not equipped with dual polarization. The polarization would reduce in great extent the amount of overestimation. This radar provides important weather information for the National Weather Service (NWS) and other media that broadcast weather information. NWS studies have shown both under and overestimation during extreme rainfall events from NEXRAD, related to the amount of rain recorded. Other rain-rate estimations derived from radar reflectivities using standard DSD models, such as Marshall-Palmer, have shown huge overestimations of rain-rate, especially because the overestimation of the number of big drops [*Schönhuber*, 2000]; in tropical climates, at least from individual studies, the number of drops tends to be more – in number – and smaller than in moderate climates. On the contrary, previous work on the Island using a Joss-Waldvogel disdrometer claimed that there is not significant difference between the computed reflectivity from the measured DSD and the one observed by NEXRAD [*Kafando*, 2003]. Therefore the use of the 2DVD in Puerto Rico will increase the confidence of the information about drops distribution in tropical climates.

This work intends to increase the reliability of DSD measurements in tropical climates, contributing to better estimation of rainfall rates. It will provide information on reflectivity

calculations to improve rainfall retrieval algorithms as well. Accurate DSD estimates will provide better attenuation correction specific to the tropics as well as improved *Z-R* relationships. It is necessary to solve discrepancies among previous precipitation estimation studies using NEXRAD.

The results of this work will present important information for the QPE algorithms that will be used in the near future within the CASA ERC. This will yield enhanced rainfall estimations, much needed for the tropical zones communities.

1.2 Literature Review

Measurement of rain intensities by remote sensing methods is of great interest for a wide field of applications [*Schönhuber*, 1995]. The reliability of those methods needs verification from point monitoring ground instruments, such as disdrometers and rain gauges. The 2DVD allows for a detailed verification of rain measurements, in some cases more detailed than traditional rain gauges. This is because of the enhanced sensitivity the 2DVD can achieve, compared to rain gauges measurements. A typical tipping bucket rain gauge will indicate just a "trace" of rain when accumulation is less than 0.1 mm. Figure 1-1 shows a widespread rain event in Graz, Austria, on October 24, 1994. Even when the event started with light drizzle around 07:04, when the disdrometer detected the first drops, the rain gauge sent the first tipping at 09:10.

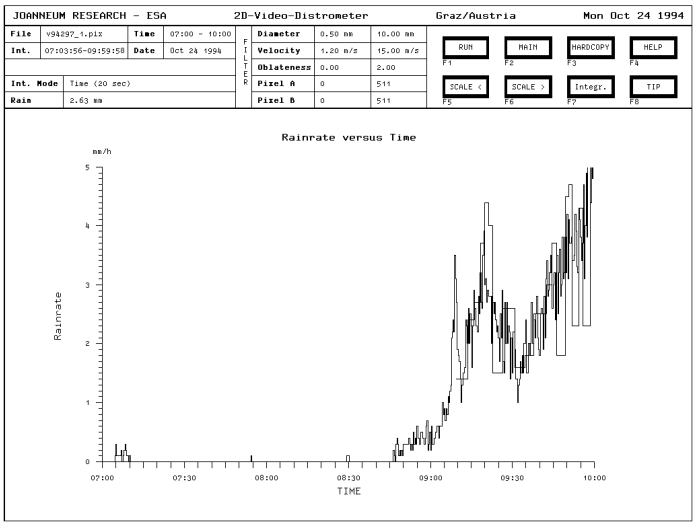

Figure 1-1 Rainfall rate vs. time during a widespread rain event in Graz, Austria, on October 24, 1994. Disdrometer data shown with 15 sec. integration interval compared to 0.1 mm tipping bucket rain gauge [*Schönhuber*, 1994].

To estimate rain that will fall over a certain area the rain-rate is derived from the DSD and the drop's diameter and terminal velocity, as shown by Kruger and Krajewski (2001) and by Doviak and Zrnić (1993). The relation of these parameters is

$$R = \frac{\pi}{6}\int_0^\infty D^3 N(D) v_t(D) dD \tag{1.1}$$

where R is rainfall rate in mm•hr^{-1}, D and v_t are the drop's diameter and terminal velocity in mm and m•s^{-1} respectively, and $N(D)$ is the DSD. Accurate measurements of these quantities are consequently needed. Both diameters and terminal velocities of falling hydrometeors can be obtained from the 2DVD accurately as demonstrated in [*Kruger*, 2001], and [*Schönhuber*, 1995, 2000]. The 2DVD software arranges drop information to construct DSD, according to Kruger.

Atlas et al. (1973) came up with a useful formula to calculate terminal velocities of water droplets that produces less than 2% error from precise measurements made by Gun and Kinzer

(1949), if the diameter of the drops is between 0.6 and 5.8 mm. This formula is the one used by the 2DVD to compute drops' vertical velocities, and is expressed as

$$v_t(D) = 9.65 - 10.3e^{(-0.6D)} \quad \text{m/s} \tag{1.2}$$

when D is in mm. The aforementioned velocities measurements were performed in stagnant air. For the 2DVD, low-wind conditions are necessary in order to obtain accurate and detailed information on drop size, velocity, and shape. High-wind conditions may introduce errors in the instrument readings.

The conversion of radar reflectivities to rainfall parameters uses standard models for DSDs [*Schönhuber*, 1995], such as the well known Marshall-Palmer DSD (MP-DSD), and others as the Joss-Drizzle (JD-DSD), and the Joss-Thunderstorm (JT-DSD) models [*Schönhuber*, 2000]. These three are exponential models of the form

$$N(D) = N_0 e^{-\Lambda D} \tag{1.3}$$

where N_0 is the scaling factor and is fixed to 8,000, 30,000 and 1,400 /m^{3}mm respectively, for the models mentioned above, and Λ is a function of the rainfall rate. The parameter Λ of the exponential distribution that fit the MP-DSD is $4.1R^{-0.21}$ mm^{-1} when the rainfall rate is in millimeters per hour. Although MP-DSD is very popular in computing rainfall rates derived from radar reflectivities measurements, actual drop sizes change significantly by geographic location, type of storm, season, and region within the storm. Regarding tropical climates, all three models mentioned produce huge overestimations of rainfall rates [*Schönhuber*, 2000]. This is due to the fact that they overestimated the number of big drops, compared to what is measured

by the 2DVD. This is shown on Figure 1-2, which depicts the DSD measured and estimation curves for the three models from experiment on Lae, Papua New Guinea, on August 30, 1995.

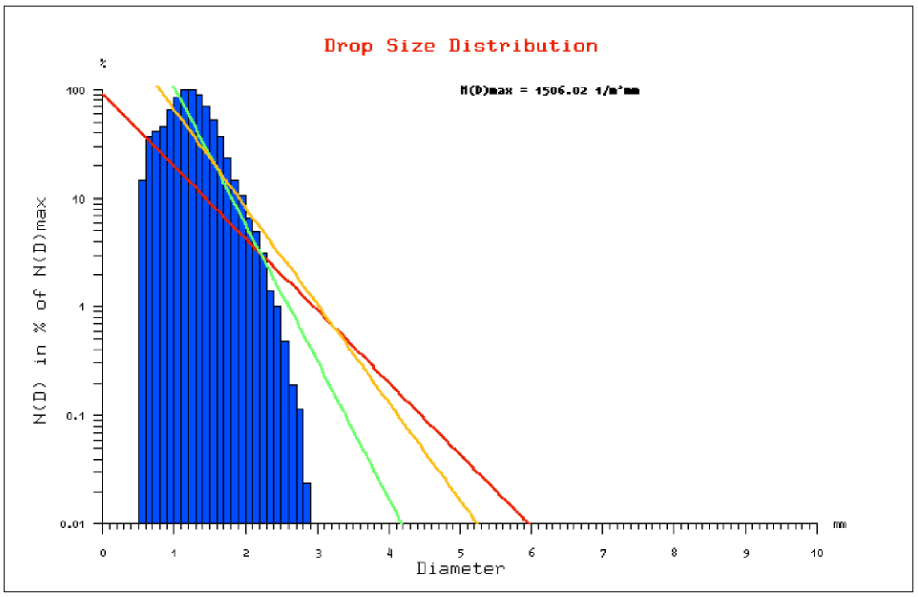

Figure 1-2 DSD out of tropical rain, recorded on 30 August 1995, 22:10-22:30, in Lae, Papua New Guinea. MP-DSD (yellow), JT-DSD (red), and JD-DSD (green) indicated. Mean *R* = 25.24 mm/hr. As shown in the figure all three methods overestimate the amount of large raindrops [*Schönhuber*, 2000].

Ulbrich (1983) proposed a general gamma distribution of the form

$$N(D) = N_0 D^{-\mu} e^{-\Lambda D} \tag{1.4}$$

to better represent the DSD. In this case $\Lambda = (3.67 + \mu)/D_0$ [*Meneghini*, 2003]. As more parameters are introduced in these equations more remotely sensed measurements are required to specify them. Since the WSR-88D is a single-polarization radar, only exponential functions can be considered, as one parameter can be fixed and the other determined. To upgrade this system the National Oceanic and Atmospheric Administration (NOAA) has planned to convert the WSR-88D at TJUA to a dual-polarization radar by the year 2007. But even when two-parameter

models reduce rainfall rates estimation errors significantly, there still exist big differences compared to measured rates [*Schönhuber*, 2000].

While comparisons in both horizontal and differential reflectivities between radar measurements and disdrometer derivations present good match, rainfall rate results are in great discrepancy [*Schönhuber*, 1995]. Differential reflectivity Z_{DR} is the ratio between the horizontal and vertical reflectivity; it is great for discriminating large drops from hail and to determine rain rates independent of the drop-size distribution; only depends on the axial ratio. In order to maeasure Z_{DR} a dual-polarized radar system is required [*Bringi* and *Chandrasekar*, 2001]; therefore Z_{DR} cannot be measured with any existing instrument in Puerto Rico.

The reason for the discrepancy mentioned is attributed to the assumptions made when converting radar reflectivities to rainfall rates. This conversion uses models for DSDs, as the ones mentioned above, whereas in converting disdrometer measurements to reflectivities actual measured DSDs are used. Radar systems convert reflectivity Z to rainfall rate R using a Z-R relationship [*Vázquez*, 2001]. This relationship is of the form

$$Z = aR^b \tag{1.5}$$

Schönhuber et al. found in 1995 that calculating reflectivities from a mean rainfall rate of 37.1 mm/hr, expected numbers were 55.08 dBZ in horizontal reflectivity Z_H and 4.36 dB in differential reflectivity Z_{DR}. Using these same numbers by inverting $Z = 200\mathrm{R}^{1.6}$ yielded more than 100 mm/hr when calculating from Z_H and 58 mm/hr when calculating from both Z_H and Z_{DR}. This confirms that even when using two-parameter models, rainfall estimations can generate considerable differences.

The WSR-88D precipitation processing system (PPS) converts reflectivity Z to rainfall rate R using a Z-R relationship [*Vásquez* and *Roche*, 2001], as stated before. On their study, Vasquez and Roche proposed new Z-R relationships, owing mostly to underestimation when rainfall accumulation for the hurricane Debbie (August 22-23, 2000) exceeds 75 mm. Furthermore, results show that there is some overestimation in about half the occurrences when rain amounts are less than 75 mm. These results were calculated using the Rosenfeld Tropical Z-R relationship, where $Z = 250R^{1.2}$. A list of NWS Radar Operational Center (ROC) accepted Z-R relationships are presented in Table 1-1. The new relationships suggested in this work by Vásquez and Roche yielded better approximations of rainfall estimation than the Rosenfeld Tropical relationship, when compared to rain gauge accumulations. The new Z-R equations where selected using the G/R ratio defined by Wilson and Brandes (1979) as the sum of the observed amounts at all gauges with rainfall divided by the sum of the radar estimates for those gauges.

TABLE 1-1 NWS Radar Operational Center (ROC) accepted Z-R relationships.

RELATIONSHIP	RECOMMENDED USE	2ND RECOMMENDATION
Marshall-Palmer $Z = 200R^{1.6}$	General stratiform precipitation	
East-Cool Stratiform $Z = 130R^{2.0}$	Winter stratiform precip. east of continental divide	Orographic rain-East
West-Cool Stratiform $Z = 75R^{2.0}$	Winter stratiform precip. west of continental divide	Orographic rain-West
WSR-88D Convective $Z = 300R^{1.4}$	Summer deep convection	Other non-tropical convection
Rosenfeld Tropical $Z = 250R^{1.2}$	Tropical convective systems	

Figure 1-3 presents the relation between the suggested *Z-R* relationships and gauge data. The problem encountered with these new relationships was that they produce rainfall overestimation for rainfall amounts of less than 76.2 mm; however for flood warnings is much more important to have proper early estimation of heavy precipitation.

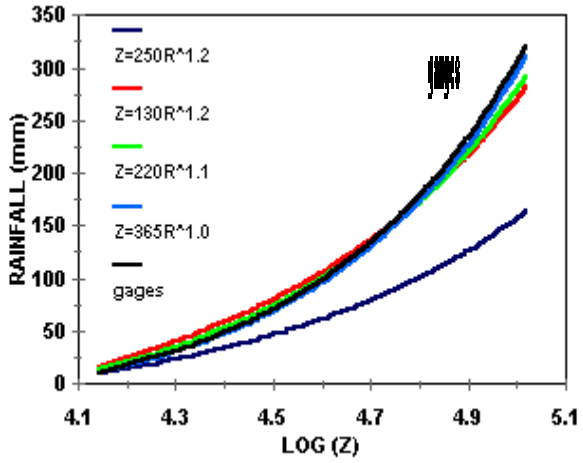

Figure 1-3 Gauges accumulations for hurricane Debbie (2000) and radar estimated rainfall vs. regressed reflectivities from alternative *Z-R* relationships for same event.

Other factors found on this study that could affect rainfall accumulation estimations are: 1) ground-clutter suppression technique used by NEXRAD's PPS, that removes power contribution from hydrometeorological targets, as it is applied to stationary echo returns, and will eliminate contributions from targets moving perpendicular to the radar beam; 2) lack of detection by the radar beam, because the scanned volume lowest height increases with the square of the range from the radar site (TJUA) and radar beam overshooting rain clouds at all ranges as TJUA is located at 850 m above sea level (see Figure 1-4); 3) a glitch on the PPS algorithm that truncates estimates at the decimal point, which would not be of much importance during short periods of

rain but prolonged accumulation estimates can produce significant errors, especially if using the User Selectable Precipitation product; and 4) radar calibration that can produce a ±1 inch of error with only a ±4 dB reflectivity error, according to Joe and Cynthia Christman (1999).

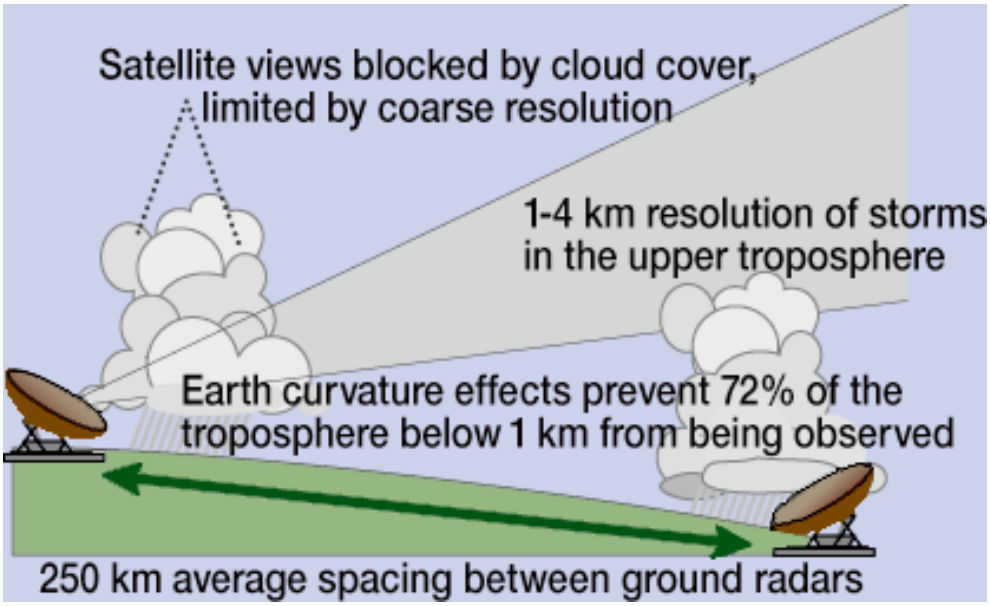

Figure 1-4 Radar beam overshooting rain clouds, worsen by Earth curvature effect.

The lack of detection by the radar beam issue, especially for Puerto Rico, is one of the key issues to be addressed by the CASA ERC [*Donovan*, 2004]. It has been proposed to install a distributed, collaborative, and adaptive network of low-power radars in strategic locations, to overcome overshooting problems, among other issues.

Regarding radar calibration, studies by Ulbrich and Miller (2000) demonstrated that the use of the default *Z-R* relation for that zone (South Carolina) with no adjustments for possible calibration offset, produces very low estimated amounts, lower by half or more [*Ulbrich*, 2001]. Comparing disdrometer data with a tipping bucket rain gauge indicated good agreement between them, implying that radar calibration was incorrect, with an average offset of -4.7 dB for the nine

storms examined. Variations on the *Z-R* relation did not yield improvements in the radar-measured rainfall unless adjustments for possible calibration offset were applied.

1.3 Summary of Following Chapters

In Chapter 2, a description is presented about the two-dimensional video disdrometer. It includes its components and their operation. It also describes the deployment in Puerto Rico of this interesting and innovative instrument. Some operational problems were found during the first months after the installation; these include communication problems, computer auto-rebooting and data remote-downloading difficulties. All are explained on this chapter.

On Chapter 3, we discuss the characterization of the drop-size distribution for the Tropical Storm Jeanne. This storm passes over Puerto Rico during September 15th and 16th, 2004. Rain for the 16th was associated with what is called the "tail" of the storm; differences were found with the 15th results, both in drop sizes and quantity. A bigger convective component was found for the 15th, which may cause most differences. It is known that noise can be introduced in disdrometer measurements, and several techniques have been developed to filter them out. This chapter introduces the reasoning behind this problems and one of these techniques, *Sequential Intensity Filtering Technique (SIFT)*, is described is this chapter.

Several instruments used for comparison are described in Chapter 4. Rain gauges are the ancillary sensors in rainfall accumulation. We provide a general description of these instruments as they provide validation for some of our results. Moreover, before introducing reflectivity values computed from measured DSDs, we present a description of the weather radar used for comparison. This is the NOAA WSR-88D radar, better known as NEXRAD, which is installed

in Cayey, Puerto Rico (radar ID is TJUA). This radar services Puerto Rico and the U.S. Virgin Islands, but its performance is diminished by the high altitude at which it is installed and the Island's topography. The reflectivity measured by NEXRAD will be compared to our computations derived from DSDs measured by the disdrometer.

The results of reflectivity computations are presented in Chapter 5. Reflectivity is calculated using diameter and DSD information obtained from the disdrometer for the event under consideration. Calculations are compared with reflectivity data provided by National Weather Service's local Weather Forecast Office; even when data available only has a 5 dBZ resolution, results produced were comparable to NEXRAD's. Chapter 6 summarizes the conclusions of the work.

2 ANCILLARY SENSORS

In order to validate and compare 2DVD measurements, different types of auxiliary sensors were used. First we used rain gauges at the NWS and San Juan International Airport (SJU) premises and later we compared the results with radar measurements. The reflectivity computations from 2DVD data and its comparisons with radar measurements are a subject of Chapter 5.

2.1 Rain Gauges

Puerto Rico is sampled by several rain gauge networks with over 170 reporting stations combined. A rain gauge is an instrument that measures rain accumulation over a certain period, depending on its capacity. Figure 2-1 shows a typical tipping-bucket rain gauge. This type of rain gauge does not need to be emptied after water has been accumulated, as it will take measurements every time rain a 0.1mm

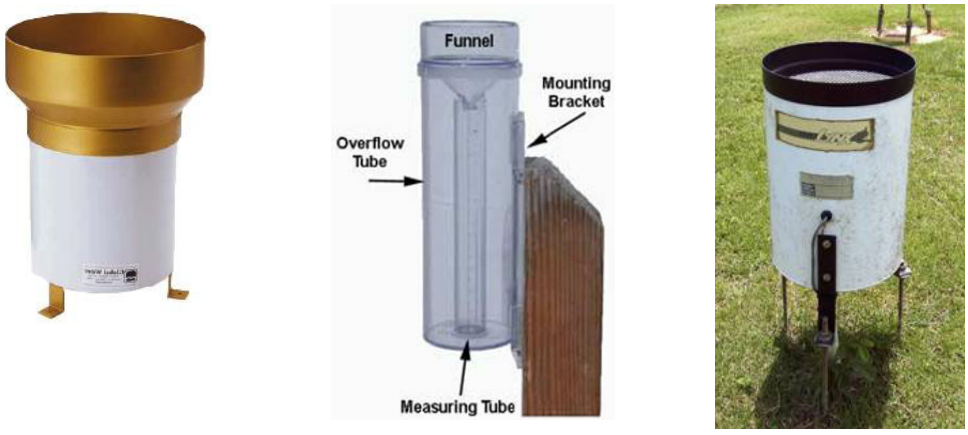

Figure 2-1 Typical rain gauges: Global Water tipping bucket, sight glass (from CoCoRaHS project), and standard.

These include mostly gauges from the United States Geological Survey (USGS), others installed on airports and those from cooperative observers' networks. USGS gauges are usually installed at river dams or other river monitoring stations, creating a lack of information when it is needed for locations in the metropolitan area. The 2DVD is not located near any of the USGS for the reason stated previously; therefore other rain gauges were considered.

The Federal Aviation Administration (FAA) has put in place an Automated Surface Observing System / Automated Weather Observing System (ASOS/AWOS). This system is a suite of sensors, which measures, collects and broadcasts weather data to help meteorologists, pilots and flight dispatchers prepare and monitor weather forecasts, plan flight routes, and provide necessary information for takeoffs and landings. SJU Airport (Luis Muñoz Marín Airport) is part of this system, and though is not at the same exact location as the 2DVD (about 1 mile west), its rain gauge gave us initial validation guidelines.

Two additional rain gauges, one 4-inch, one 8-inch, are located at NWS premises, right by the 2DVD location. However, data collection from these is done manually, creating deficiencies in data management and availability. Consequently we were forced to use data from the ASOS station which is available online and collected automatically at least every hour.

2.2 WSR-88D Radar

Located in the eastern-central part of the Island is the Weather Surveillance Radar-1988 Doppler (WSR-88D), also known as NEXRAD. For NWS purposes this radar is identified as TJUA.

The WSR-88D precipitation processing system (PPS) converts reflectivity (Z) to rainfall rate (R) using a Z-R relationship. Because of the complex mountainous terrain, the TJUA radar detects localized ground clutter over several areas. A ground clutter suppression technique is used to filter those non-meteorological, ground-based targets that otherwise would produce false reflectivity echoes affecting the PPS algorithm estimates. Ground clutter suppression may also affect rainfall accumulation by removing power contribution of hydro-meteorological targets. This technique is applied on stationary echo returns, thus hydro-meteorological targets moving perpendicular to the radar beam may be filtered as well.

Another contributing factor to inaccurate precipitation estimation is the lack of detection by the radar beam. As the radar beam samples the atmosphere, the scanned volume lowest height increases as the square of the range from the RDA. The elevation angles of the radar beam used by the PPS to estimate rainfall rates are the lowest four tilts: 0.5°, 1.5°, 2.4°, and 3.4°. In addition, the WSR-88D site (TJUA) is located on a mountain top at an elevation of 2,900 feet above sea level. Thus, the effect of radar beam overshooting rain clouds at all ranges would contribute to additional radar underestimation. Figure 2-2 illustrates the minimum height of NEXRAD's main beam coverage across Puerto Rico. It is noted from here that over the western part of the Island its coverage starts above 2,500 m.

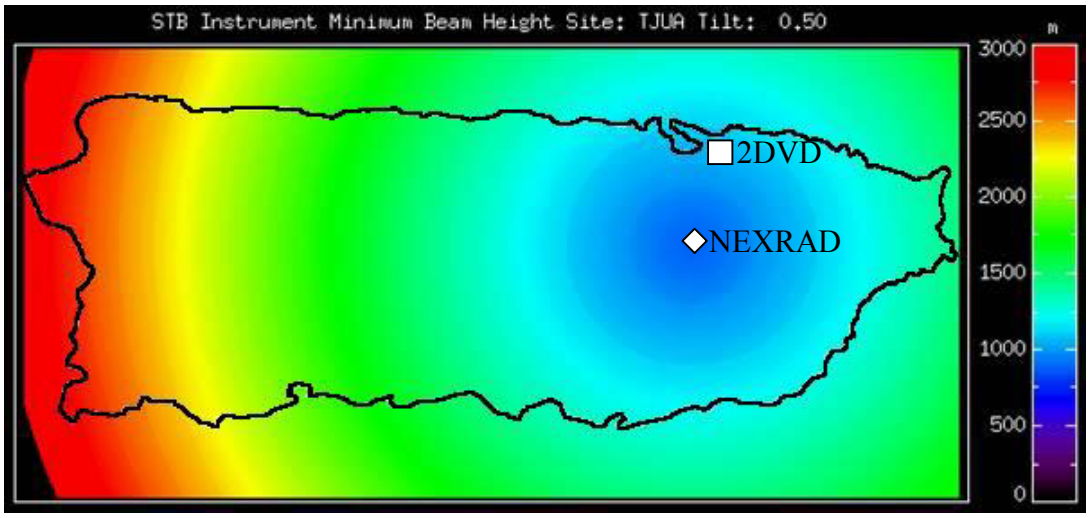

Figure 2-2 NEXRAD minimum beam height in meters along the island of Puerto Rico [*Donovan*, 2004].

3 Two-Dimensional Video Disdrometer (2DVD)

The 2DVD was developed by Joanneum Research from Graz, Austria, and the ESA/ESTEC (European Space Agency / European Space and Technology Centre). Joanneum Research, with 15 research units, is one of the largest non-university research institutions in Austria. Additionally, students of the Technical University of Graz have also contributed to its development.

A 2DVD is a precipitation gauge, working on the basis of video cameras. This optical device is utilized for raindrop size, shape and velocity measurements. It detects shadows made by passing drops using light and line-scan cameras. The information obtained allows for computations of: drop size distribution (DSD), oblateness, equivolumetric diameter, rainrate, and velocity (horizontal and vertical).

The advantages of this two-dimensional video configuration are several. First it avoids the problem of counting splashes of drops as other individual drops. Second, the special arrangement of the cameras in different planes allows for the actual measurement of fall velocities.

3.1 Main Components and Operation

3.1.1 Sensor Unit

The Sensor Unit houses the two cameras, two light sources, and several mirrors (see Figure 3-1(a) and (b)). Mirrors are used to deflect light as lamps are not directly in front of the cameras.

Each camera-lamp pair is orthogonal to the other, providing the two-dimensional aspect of the measurement, as shown in Figure 3-2.

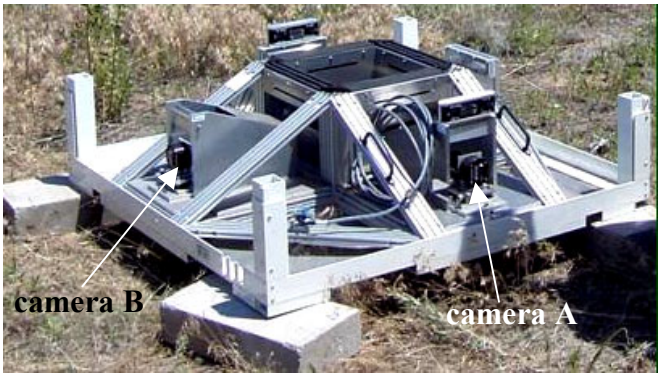

(a)

(b)

Figure 3-1 Sensor Unit without aluminum covers; (a) shows camera locations and (b) shows lamp locations.

When a raindrop falls into the measuring area, cameras 1 and 2 detect the drop shadow. The two orthogonal projections provide 3D raindrop shape information that is used to describe the raindrop. The sensor unit operates at a frequency of 34.1 kHz, taking drop measurements every 29 microseconds approximately.

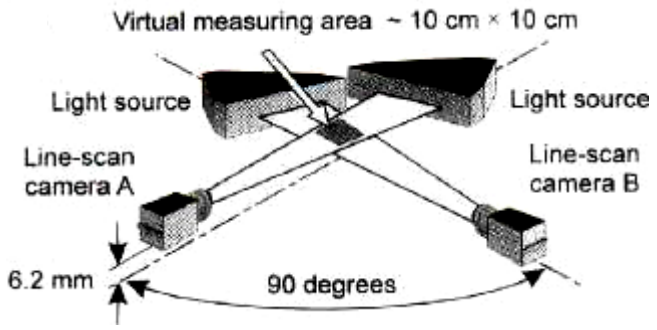

Figure 3-2 Sketch of Sensor Unit components [*Schönhuber*, 1994].

3.1.2 Outdoor Equipment Unit (OEU)

The OEU (see Figure 3-3) consists of an embedded computer (PC), power supply – to power lamps and cameras – and connections for power and video signals from the cameras. It receives those video signals from cameras, pre-processes raw data, and runs software for data acquisition and plane alignment. It also provides connections for a keyboard and monitor to access its computer.

Every 3 seconds, data are "packaged" by the OEU PC and transmitted via TCP/IP to the Indoor User Terminal, a third component that is described below.

Figure 3-3 OEU, open at left, closed at right (back).

3.1.3 Indoor User Terminal (IUT)

The IUT is a regular PC that receives the pre-processed data from the OEU and performs the final computations. It also provides display of these calculations via a proprietary software called VIEW_HYD. An image of the software display is shown in Figure 3-4. IUT is commonly named indoor computer or indoor PC (personal computer).

Several parameters are computed from measurements taken by the Sensor Unit, including rainfall rate, drop size distribution (DSD) and oblateness. Other measured parameters are compared with calculations from well-known models.

To begin with, consider rainfall rates. These are not based in time as one would expect, but in quantity of rain in a given amount of time. The amount of rainfall rate displayed will be the rain accumulation for the last 30 minutes since the last 0.1 mm increment.

Another parameter displayed by VIEW_HYD is the DSD. It is calculated using

$$N(D_i) = \frac{1}{\Delta t \Delta D} \sum_{j=1}^{M_i} \frac{1}{A_j v_j} \left[\frac{1}{m^3 mm} \right] \tag{3.1}$$

where Δt is the integration time interval in seconds, ΔD is the width of size class in mm, A_j is the effective measuring area of drop j in m^2, v_j is the velocity of drop j in $m \cdot s^{-1}$, I is the drop size class, j is the single drop, M_i is the number of drops in class I during Δt, and D_i is the diameter of class i.

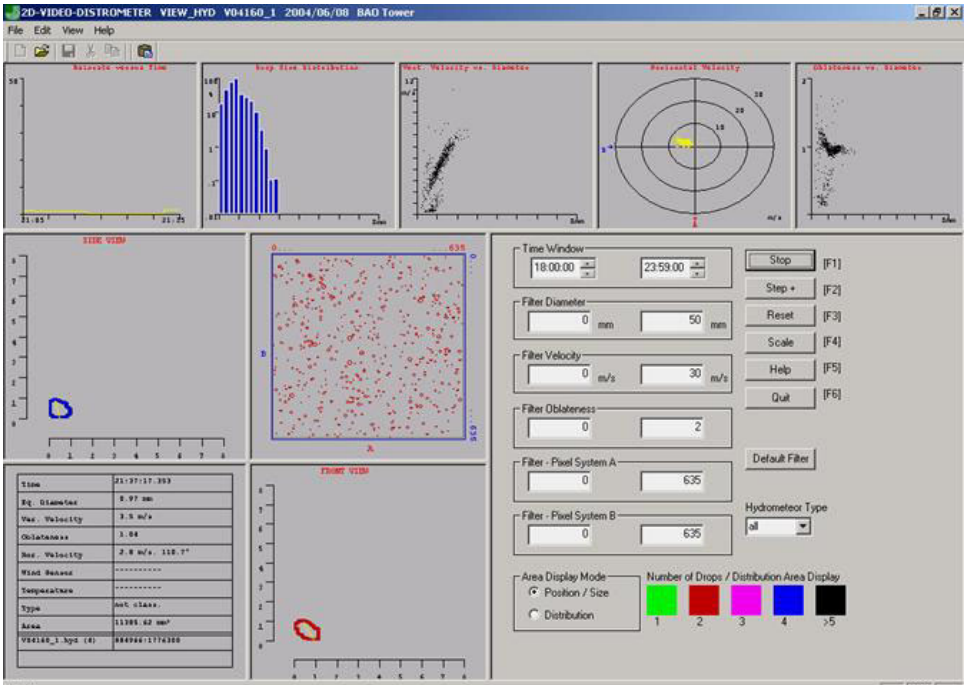

Figure 3-4 Image of the VIEW_HYD software that provides rainfall and raindrops information.

Regarding vertical velocity, as stated before, is measured by the difference in distance between light planes, but it also is compared with computed velocity determined after Atlas *et al* (1973). This relation is given by

$$v(D) = 9.65 - 10.3e^{-0.6D} \tag{3.2}$$

where v is the velocity in m•s^{-1} and D is the diameter in mm.

One important parameter computed by the 2DVD is the oblateness, which is defined as the geometrical mean of the height/width (H/W) ratios of a raindrop's front and side view. As the drop is actually measured by the cameras, oblateness is not estimated from the diameter as done

by other models developed by Pruppacher and Beard (1970) and Poiares Baptista (1992). The equations for oblateness mentioned are

$$\frac{H}{W(D)} = (1.03)(0.124)\frac{D}{2}$$ Pruppacher and Beard (1970)

$$\frac{H}{W(D)} = (1.064)(0.07046)D(0.00072619)D^2$$ Poiares Baptista (1992)

3.2 Sites Evaluation and Deployment in Puerto Rico

Previous to the installation of the 2DVD in Puerto Rico, I traveled to Colorado State University (CSU) at Fort Collins, Colorado, to learn about the operation of the equipment and participate in several measurement campaigns. These were performed in conjunction with CHILL radar – CSU's S-band research radar – and a NOAA X-band radar.

After that experience we started evaluating sites for the 2DVD deployment in the Island. Following sections will describe the evaluation of those sites and the final decision on the site selected.

At the beginning we planned to install the 2DVD in the western part of the Island for two principal reasons: 1) it is well known that in the west it rains very regularly with strong rain events from May to December, and 2) a western location will be closer to our campus for traveling to calibrate and work with the instrument. Regarding the first reason stated, Figure 3-5 shows the daily precipitation in a decade composite for the Mayagüez area. Amazingly the daily accumulation is close to the amount of rainfall in the rainforest region. As for the second reason public transportation in Puerto Rico is very scarce, especially in the western part, and not all

students possess private automobiles to travel back and forth the university campus. As a direct consequence of the public transportation limitation, the traffic is heavy in our roads, what would cause spending resources (time, money) to complete this task.

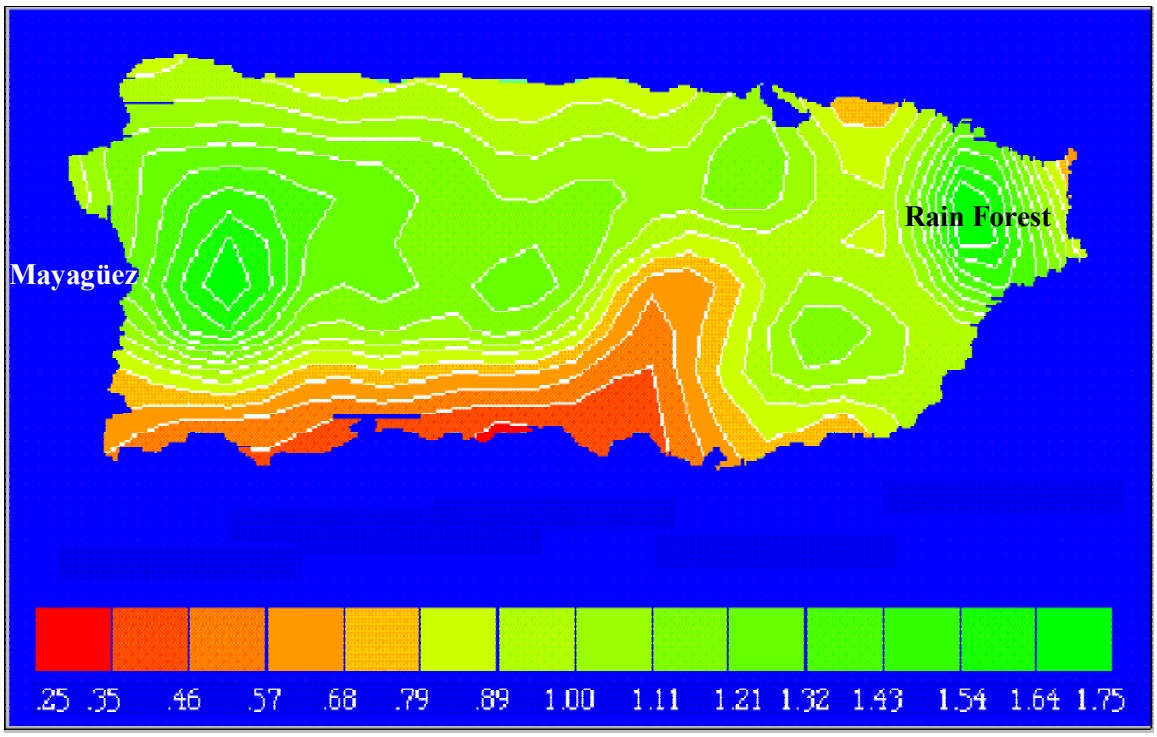

Figure 3-5 95%-ile values of daily precipitation (inches) derived from a composite of monthly average rainfall from 1980 to 1989. After Carter *et al.* 1997.

We evaluated two possible sites, where the University of Puerto Rico – Mayagüez is the proprietor. One of them is at "Finca Montaña" in Aguadilla and the other is at the Agricultural Experimental Station in Isabela. Table 3-1 shows details for each site.

TABLE 3-1 Site Evaluation Details

Site Options	Finca Montaña, Aguadilla	Agricultural Experimental Station, Isabela
Location	18°28.465'N, 67°07.267'W (NAD 27)	18°27.767'N, 67°03.163'W (NAD 27)
Site Details	👍 Air conditioning available • working but need to change to manual as power ON is not automatic after power failures 👍 Telephone line available • actually disconnected as not in use • one week in advance for re-installation request • private university campus very close, so high-speed data circuits should be available in the area if needed 👎 No employees on site 👎 Needs maintenance contract 👎 Strong easterly winds were present during visit	👍 Area besides weather station available 👎 Land east of weather station may need leveling 👎 Building located more than 250 ft away 👎 LAN, power and indoor space available are at this distance 👍 Very well maintained area 👍 Employees on site makes area safer 👍 Rain gauge and weather instruments on site

Figure 3-6 shows photographs at both locations of the first two proposed areas. However, these propositions were abandoned as it is known that NEXRAD coverage is poor in the western part of the Island, one of the primary challenges to the CASA project. Next it was decided that the search area should be were NEXRAD coverage is known to be accurate.

(a) (b)

Figure 3-6 Proposed areas at (a) Aguadilla site and (b) Isabela.

Being NWS a partner to the CASA ERC, it came naturally to consider their location as an alternative for the 2DVD installation. Though NEXRAD covers from 4,000 feet up at this location, it provides accurate and reliable information for this metropolitan part of the Island. After some evaluation of their premises, NWS management approved for the installation and employees were very helpful in the whole process. Figure 3-7 illustrates the three possible locations considered at NWS and Figure 3-8 the final installation.

At first the area by the ASOS station at the airport was considered, but airport's security constraints make the logistics of installation and regular visits very difficult. This was understandable as this station is by the runway. Another key factor was the lack of a communication link between NWS and the station site. There was no space at the site to install the IUT so it would have been necessary to use the NWS location for that purpose, therefore there were no simple way of connecting to it.

(a)

(b)

(c)

Figure 3-7 Three areas considered for 2DVD installation on or close to NWS premises: (a) ASOS station at San Juan International Airport; (b) NWS main building roof; and (c) NWS yard. Location (c) was selected for the final installation.

Another location considered was NWS main building's roof, but blocking from big air conditioning machines and other parts of the buildings would create wind deflections and turbulences not desirable for our measurements. It has been stated that 2DVD provides accurate

and detailed information when working under low-wind conditions. Therefore the roof consideration was abandoned.

Figure 3-8 Picture of 2DVD's sensor and OEU completed installation with personnel from NWS. IUT was installed at the building at the far right (red roof).

After these considerations it was found that the ground surroundings had enough clearance from buildings, trees and fences that encircle the installation area. Additionally, a small building used by NWS hydrologists was within reasonable distance to install the IUT and to connect power. Finally, NWS rain gauges and other weather sensors were located in the same area, providing for measurements validation.

3.3 Comparison with traditional rain gauge

Considering the 2DVD as a precipitation gauge, it was reasonable to compare its measurements to a traditional rain gauge. The rain gauge information was obtained from the ASOS station described in Section 2.2. An initial comparison was performed during Tropical Storm Frances affecting Puerto Rico on August 30-31, 2004. This comparison set basis to rely in 2DVD data as a means of measuring precipitation parameters.

ASOS information is available in an hourly basis, so 2DVD rain rate was converted to hourly accumulation. Rain rate and DSD information is obtained using a program provided by Colorado State University, called FIRM_DSD. This program reads 2DVD proprietary-formatted files and converts them to text files with the following information: time, diameter range, DSD values, and rain rate. For each minute (time periods are user-defined in terms of seconds) a DSD value is reported for each diameter range, varying from 0 to 0.25 mm to 10 to 10.25 mm. Additionally, the computed rain rate for each minute is provided. The minute values were summed for an hour and multiplied by the hour to change the millimeters per hour to millimeters (e.g., accumulation).

First we evaluated the performance of FIRM_DSD compared to what was displayed by VIEW_HYD. Results from FIRM_DSD shown in Table 3-2 were very close to VIEW_HYD as expected, as the instrument and FIRM_DSD software had been in use for some time.

TABLE 3-2 FIRM_DSD performance evaluation.

Total Precipitation	Aug. 30, 2004	Aug. 31, 2004
Total precipitation VIEW_HYD	4.28 mm = 0.17 in	4.60 mm = 0.18 in
Total precipitation FIRM_DSD	4.2755 mm	4.6031 mm

Next we compared 2DVD with ASOS rain gauge daily accumulation during Frances. Figure 3-9 and Table 3-3 shows detailed results of the comparison. Results yielded less than 0.5% difference between the two instruments, providing the confidence to start working with larger data sets towards our DSD characterization goal.

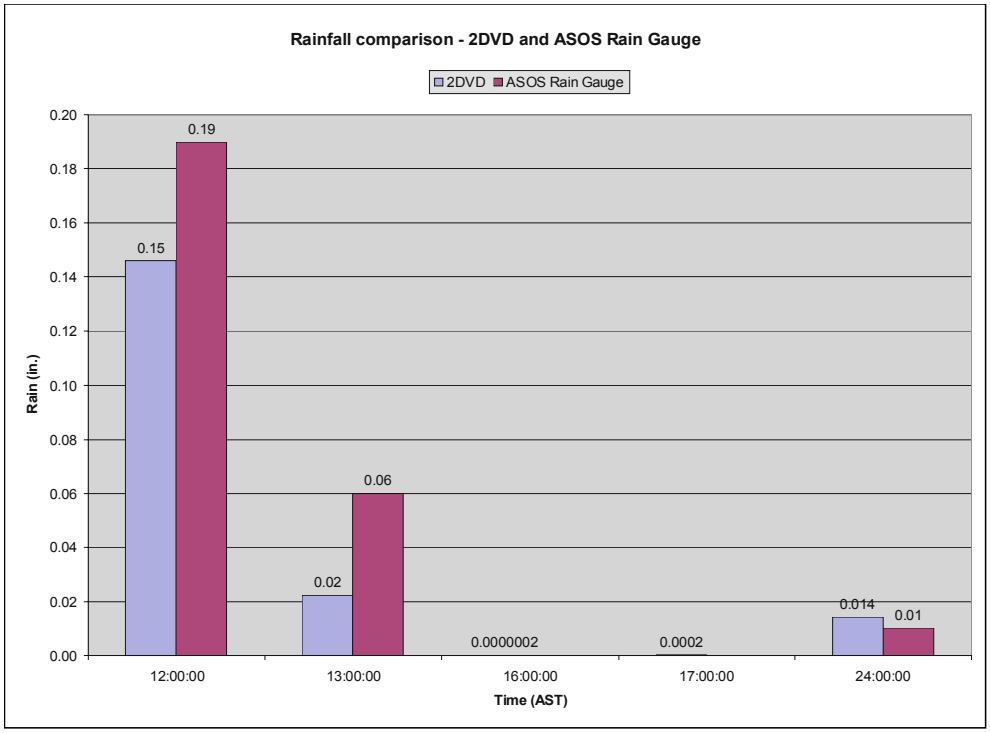

Figure 3-9 Comparison between 2DVD and ASOS hourly precipitation accumulation for Aug. 30, 2004 during Tropical Storm Frances.

TABLE 3-3 Comparison between 2DVD and ASOS rainfall accumulation during Tropical Storm Frances, August 30-31, 2004.

Total Precipitation	Aug. 30, 2004	Aug. 31, 2004
Total precipitation 2DVD (mm)	4.6369	4.2448
Total precipitation 2DVD (in)	0.1826	0.1671
Total precipitation ASOS(in)	0.25	0.22
% difference	0.38	0.40

Nevertheless our good results, several problems were found after the installation of the 2DVD which resulted in data loss and time consuming trips to the instrument. These are described next to inform and try to prevent problems for future work.

3.4 Operation problems encountered

3.4.1 Remote monitoring and data downloading

Original plans for monitoring the 2DVD were to use a commercial network computing software that allows viewing and fully-interacting with one computer from any other computer on the Internet [RealVNC web site]. This was planned because of the long driving distance between the University campus and the NWS office – around two and a half hours – which prevented us from regularly monitoring 2DVD and downloading data. Problems started with firewall and information systems security issues at both sites, but mostly at NWS, as it is part of the U.S. federal government and security is a priority after 9-11 events. Remote connections can only be established from the NWS out, but not into their network.

For several months this practice took place, connecting from IUT to our computer or to Colorado State University network, as their firewall did not disconnect the communication as easily as ours (Mayagüez campus). This was done by us or by the very cooperative personnel at NWS when we requested to. However, when IUT started presenting what looked as communications problems with OEU, it was believed that new IP addresses could be "confusing" the internal TCP/IP transmission, causing the system to fail and consequently to loose valuable data. It was the recommendation of the manufacturer to stop downloading data remotely, to avoid more system failures, which caused the schedule of more regular trips to the equipment for monitoring stability and to retrieve archived data.

3.4.2 Communication problems between computers

Together with the previous problems, IUT computer started presenting messages regarding communication problems between it and the OEU. Most of the times the action taken by the computer was rebooting itself, with the opinion of the majority of people involved in the project that when loosing communications it created a major system error and caused the computer to restart itself. When it booted and there was nobody there – which was the case most of the times – the system did not 'log in' itself and as a result the data collection program did not start. Apparently this happened in a two-week interval of time, approximately. The solution to this, regardless of known security issues, was to eliminate the need for logging in when starting up the computer. Security was not a major concern because access to NWS premises is limited to employees and citizens or press requiring weather information. In addition the building were the IUT was located was not used frequently or by many people.

Kruger and Krajewski (2001) found several causes for the 2DVD to fail. These include some that have been corrected with newer software versions, such as problems synchronizing IUT and OEU clocks, which caused the IUT to lock up. Other problems they found were heat-related problems and blocking of light planes by insects or small objects; this last problem is inherent to the equipment design. Because of these issues they recommend not to operate the instrument unattended for more than four to five days. As we were not able to monitor the instrument with this frequency, we were not able to identify what the specific problem was causing the system to shutdown.

Nevertheless, we knew that the coaxial cable connecting the indoor and outdoor computers was a lot longer than needed. Distance between OEU and IUT was in the order of 100 feet and communications cable shipped with the instrument was a 1000-feet reel. We were asked by the manufacturer not to cut it and make new connectors, because some communication problems could arise. Instead, after trying several indoor computer configurations, the manufacturer shipped a new cable with the length required. After replacing the coaxial cable continuous working time without systems failures was considerably extended, from about one or two weeks to one month or more.

3.4.3 Human factor

One thing to consider, even when it is not technically related, is the human presence near the indoor computer. When analyzing possible causes for the computer to crash, it was found that the power button of the computer was very sensitive and at the same time very easy to hit with the foot as the PC's CPU was on the floor. Space available at the IUT location is limited and there is another computer beside it, on the same table, as observed in Figure 3-10.

Figure 3-10 IUT (indoor PC) installation inside NWS building.

Another possibility, besides hitting the power button, is a combination of losing communication with the OEU and the presence of a NWS employee. When the communication is lost between the outside and indoor computers a "beep" sound is emitted from the indoor PC. It could be that a person working in the area is annoyed by the beeping or trying to help solving the problem, he or she can power off the computer. We tried to turn off the beep but did not find a way, so we could not control that event. For the protection of the power button we moved the CPU in a way that the switch was protected from any accidental punch.

3.4.4 Summary of recommendations

After dealing with the aforementioned problems, several recommendations are presented. It is hoped that these will help with future experiments using this instrument.

First install the instrument in a place with easy access to monitor it regularly, at least once a week or every other week. There are still several unknown causes to the failures experienced that it is not suitable to operate the instrument unsupervised for long periods of time. Regarding the indoor PC, place it where its power button is not exposed to accidental hits. When possible place PC on top of a desk or table to avoid unintended thumps from people's feet.

In terms of communications between OEU and IUT, install coaxial cable with the required length, trying not to exceed 200 feet. We have been told by Dr. Bringi that problems occurred in another experiment when exceeding this length.

Until further investigation and trials it is not recommended to download data from IUT using remote techniques, such as ftp (File Transfer Protocol). This has been a suggestion from the

manufacturer but it is also suggested to investigate if that was really causing communication failures between both computers.

4 DSD characterization for a tropical storm event

4.1 Procedure

DSD information is obtained using the FIRM_DSD program described in Section 3.3, provided by Colorado State University.

To characterize DSDs, two parameters were computed, according to Bringi and Chandrasekar (2001): the mass-weighted mean diameter, D_m, and the normalized intercept, N_w, using

$$D_m = \frac{\int D^4 N(D) dD}{\int D^3 N(D) dD} \text{ (mm)}, \tag{4.1}$$

$$N_w = \frac{(4)^4}{\pi \rho_w} \left(\frac{10^3 W}{D_m^4} \right) \text{ (drops * mm}^{-1} \text{ * m}^{-3}\text{)}, \tag{4.2}$$

Both parameters are used to normalize DSDs, reducing the scattering of data points. This is useful in comparing the shapes of distributions with widely different rain rates [Bringi, 2001]. Other characterizations use the median volume diameter D_0 and the N_0 parameter. For an exponential DSD D_0 is defined such that drops less than D_0 contribute to half the total rainwater content W, e.g.

$$\frac{\pi}{6} \rho_w \int_0^{D_0} D^3 N(D) dD = \frac{1}{2} \frac{\pi}{6} \rho_w \int_0^{\infty} D^3 N(D) dD = \frac{1}{2}(W) \tag{4.3}$$

In order to compare to results from similar studies, stratiform rain was defined as that with R greater than 0.5 mm/hr and standard deviation from R less than 1.5 mm/hr. Conversely

convective rain was defined as that with R greater than 5 mm/hr and standard deviation from R greater than 1.5 mm/hr.

For September 15, 2004, 712 minutes of data were recorded by the 2DVD, whereas for September 16th, 970 minutes were available for analysis. To reduce computing times, data was averaged every 2 minutes, for DSD characterization analysis, thus 356 data points were used for the 15th and 485 for the 16th.

4.2 D_m and N_w results

Table 4-1 summarizes values found for both $<D_m>$ and $\log_{10}<N_w>$; these were as expected with maritime characteristics, even when convective rain results were not consistent with previous studies made in the Island. These studies will be discussed later.

TABLE 4-1 D_m and $\log_{10}<N_w>$Results Summary

DAY/RAIN TYPE	$<D_m>$ [mm]	$\log_{10}<N_W>$
Sep. 15, 2004 stratiform	1.14	4.19
Sep. 15, 2004 convective	1.38	3.96
Sep. 16, 2004 stratiform	0.98	4.61
Sep. 16, 2004 convective	1.04	4.80
whole event-stratiform	1.12	4.51
whole event-convective	1.30	4.35

Figure 4-1(a) shows results from previous studies on stratiform rain parameters as well as findings from this work (see San Juan marker). Interestingly it shows results of the summer of 2004 studies in Colorado, where we briefly participated. Regarding stratiform rain, about 50% of data points were classified as this type on the 15th of September, while about 33% were selected on September 16th; for the combined data set a total of 40% of points were classified as stratiform.

On the other hand, as opposed to findings by Ulbrich, Petitididier and Campos (1999) in a mountainous region of the island, when continental properties were found in the DSDs, log10<N_w> versus <D_m> plot shows characteristics similar to the Maritime Cluster (see Figure 4-1(b)).

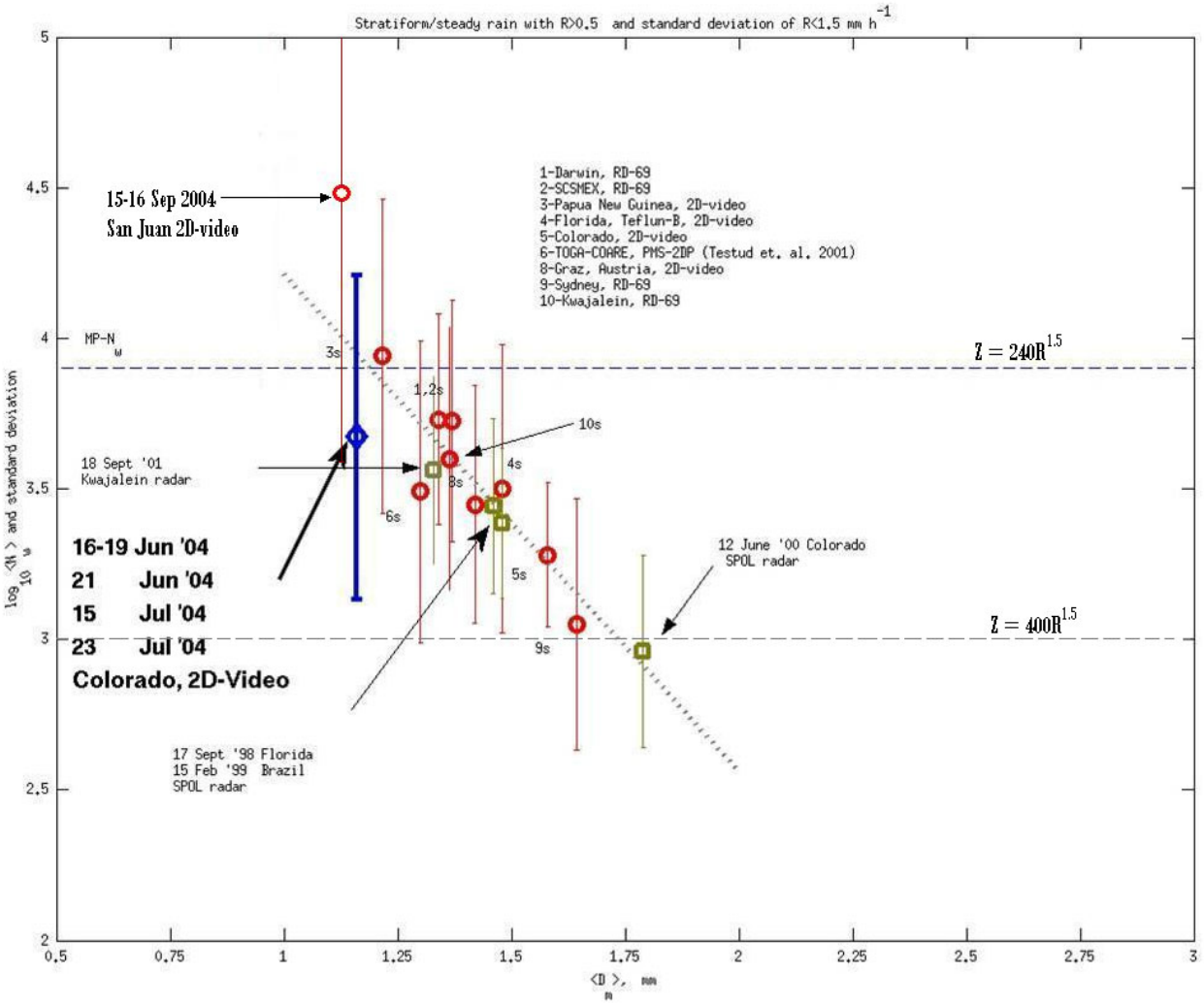

Figure 4-1 (a) The value of log10<N_w> (with 1s std dev bars) versus <D_m> from 2DVD data (numbered open circles) and dual-polarization radar retrievals (open squares as marked) for stratiform rain. Dotted line is the least squares fit. Note that N_w is the 'normalized' intercept parameter and D_m is the mass-weighted mean diameter of a 'normalized' gamma DSD.

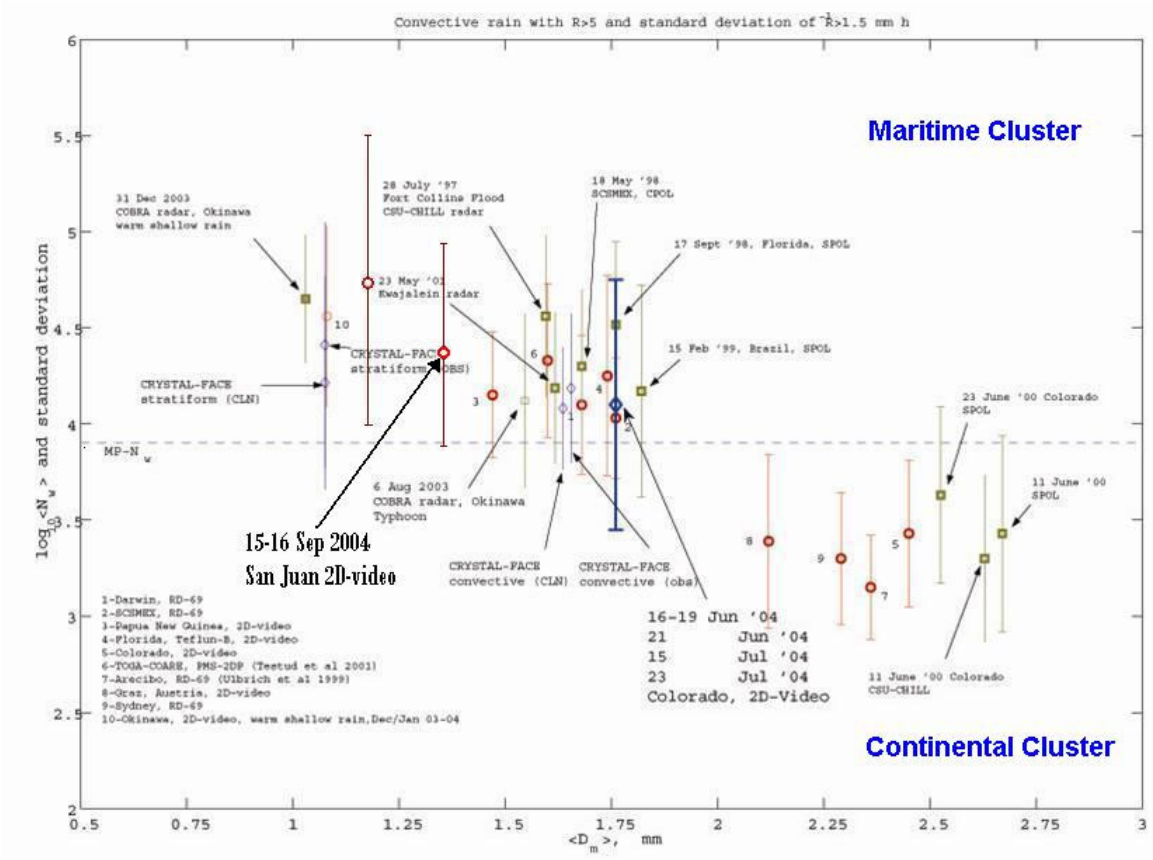

Figure 4-1 (b) As in (a) except data for convective rain. Note that N_w is the 'normalized' intercept parameter and D_m is the mass-weighted mean diameter of a 'normalized' gamma DSD.

Since less than 20% of data points were classified as convective rain in any of the two days, these results require further comparison to future events, in order to make them statistically significant.

Next pages present scatter plots and histograms (Figures 4-2 to 4-6) characterizing DSDs for the event under consideration. Noticeable is the smaller number of points classified as convective, with little less than 18% when considering the event as a whole. Classification parameters for stratiform and convective rain were kept at values stated in Section 4.1.

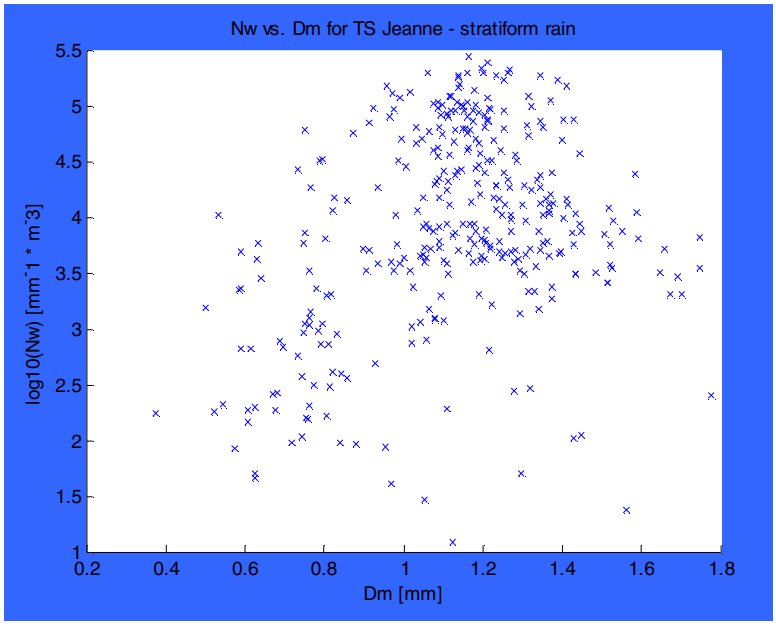

(a)

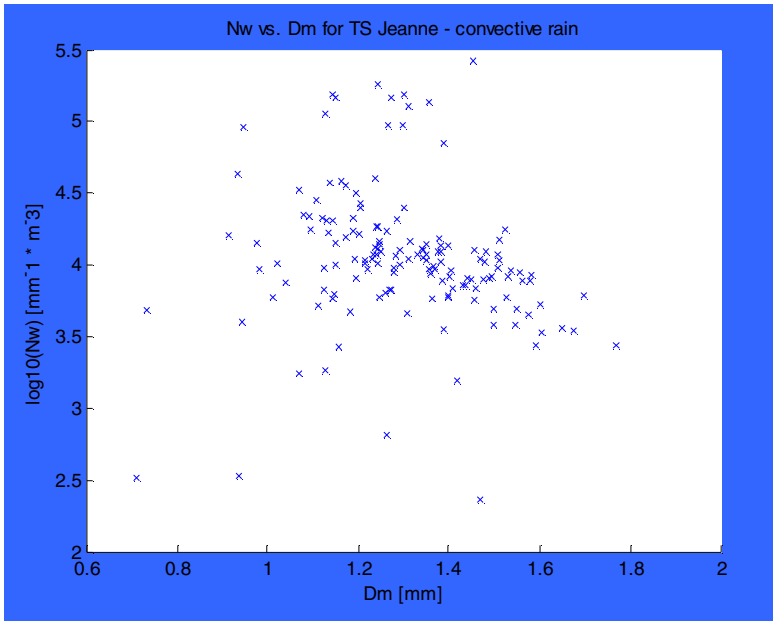

(b)

Figure 4-2 $Log_{10}(N_w)$ vs. D_m scatter plot for the Tropical Storm Jeanne, affecting Puerto Rico on September 15-16, 2004. (a) Stratiform type rain; (b) convective.

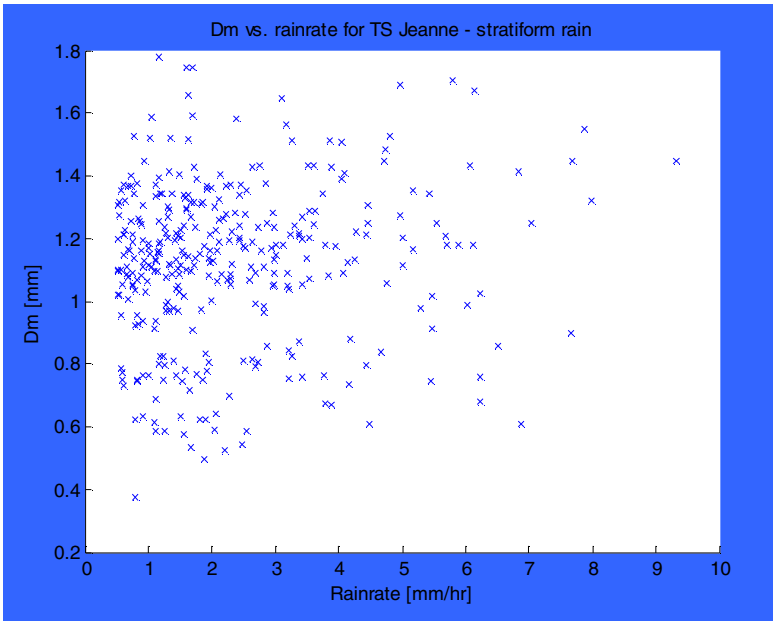

(a)

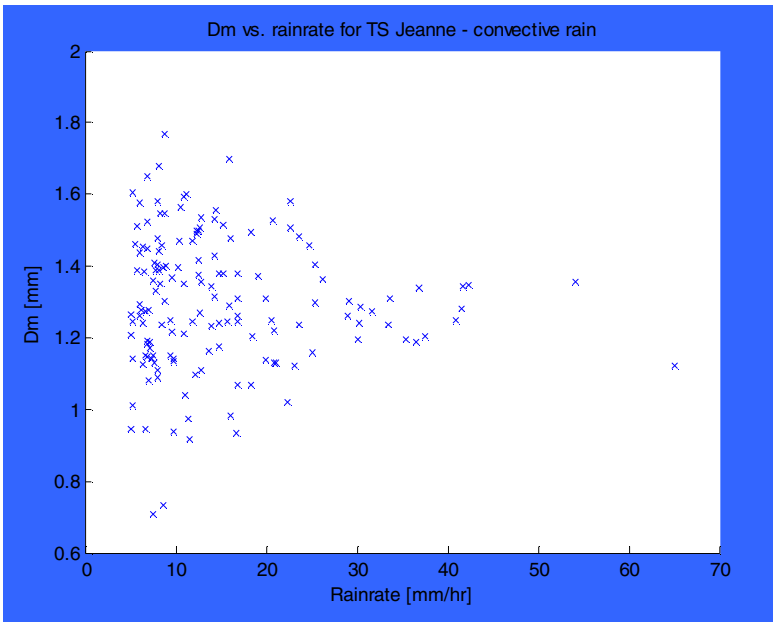

(b)

Figure 4-3 D_m vs. rain rate scatter plot for the Tropical Storm Jeanne, affecting Puerto Rico on September 15-16, 2004. (a) Stratiform type rain; (b) convective.

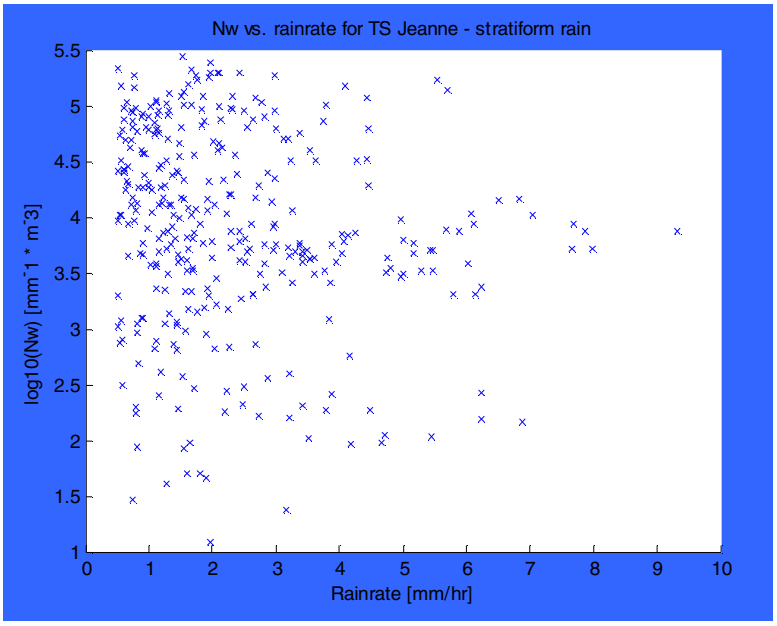

(a)

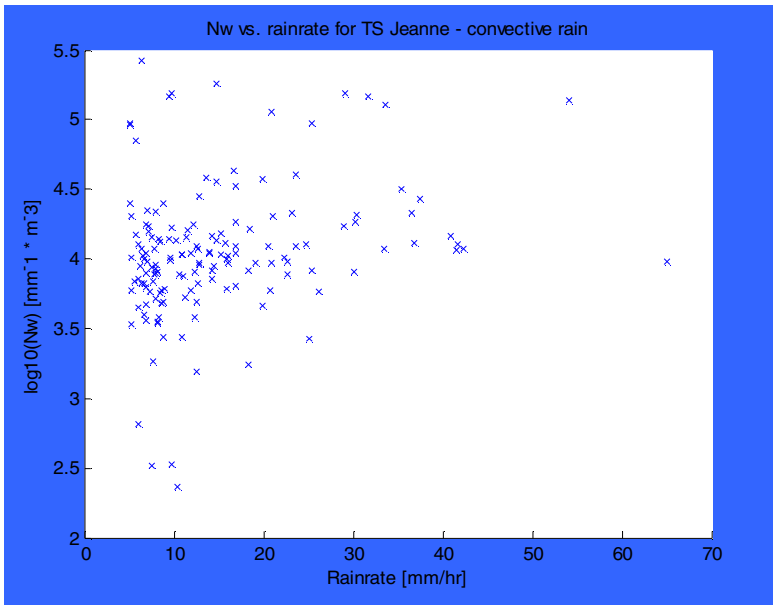

(b)

Figure 4-4 $Log_{10}(N_w)$ vs. rainrate scatter plot for the Tropical Storm Jeanne, affecting Puerto Rico on September 15-16, 2004. (a) Stratiform type rain; (b) convective.

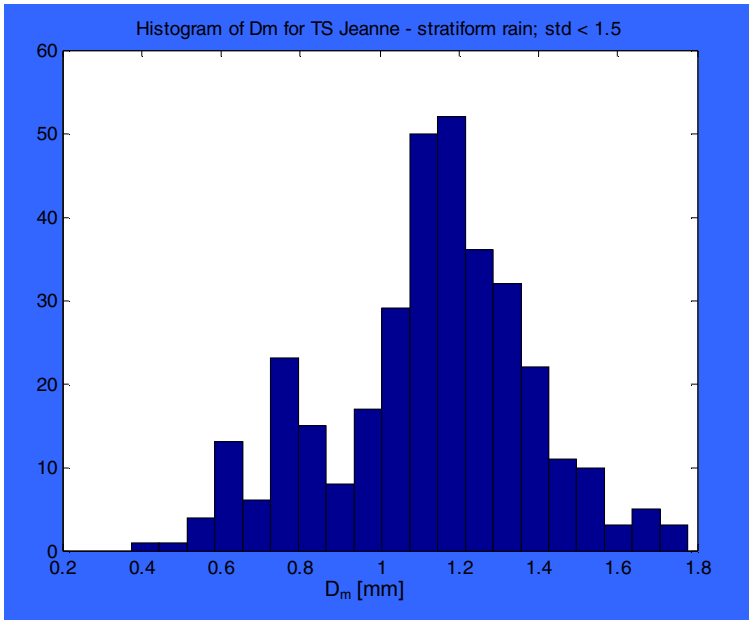

(a)
mean = 1.1247 mm, mode = 1.1812 mm

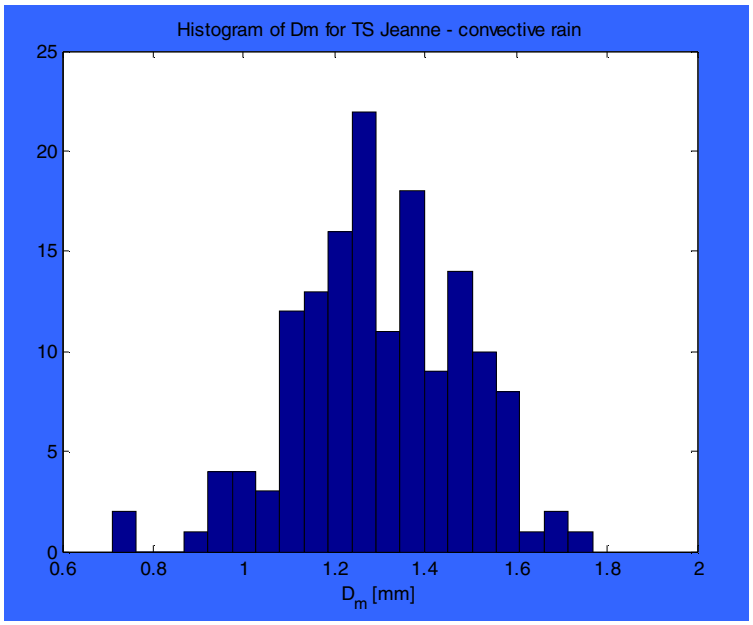

(b)
mean= 1.2988 mm, mode= 1.2656 mm

Figure 4-5 D_m histogram for the Tropical Storm Jeanne, affecting Puerto Rico on September 15-16, 2004. (a) Stratiform type rain; (b) convective.

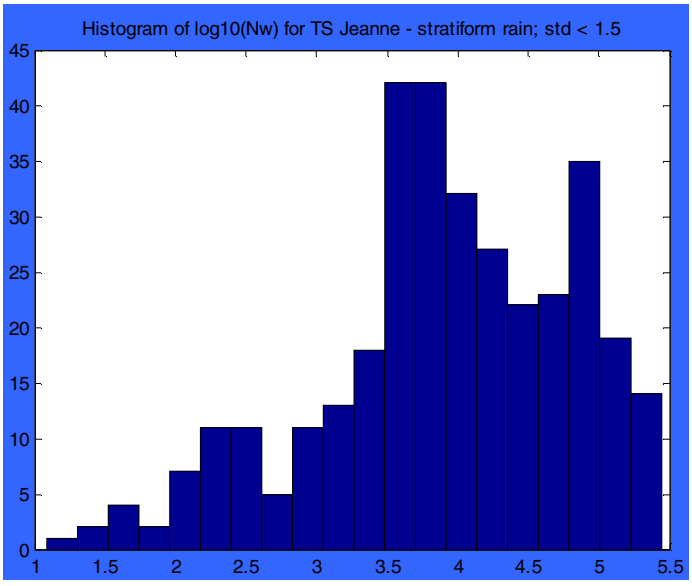

(a)

mean=4.5119, mode=3.59, 3.8074

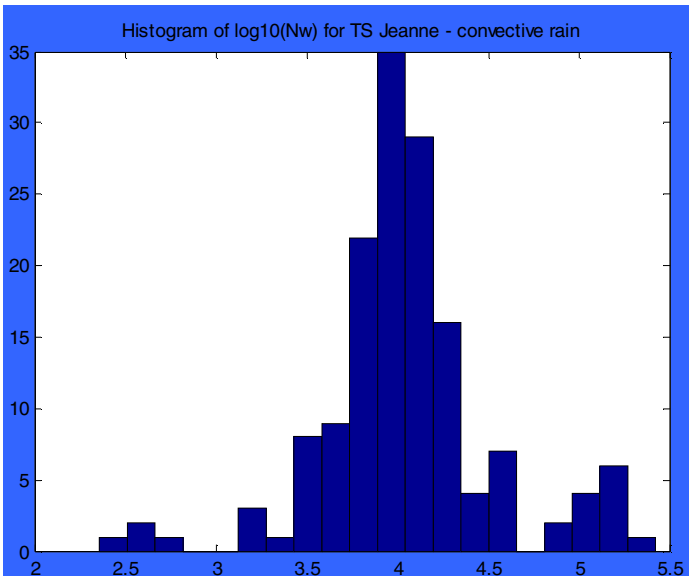

(b)

mean=4.3505, mode=3.9690

Figure 4-6 $Log_{10}(N_w)$ histogram for the Tropical Storm Jeanne, affecting Puerto Rico on September 15-16, 2004. (a) Stratiform type rain; (b) convective.

When comparing these results to preliminary results from last summer in Colorado – provided by CSU – mean values of D_m differ around 0.45 mm and values of N_w around 0.3 drops•mm^{-1}•m^{-3} (Colorado study used D_0 instead of D_m but according to Bringi and Chandrasekar these values are close). These confirm disparities in weather types, being at very different geographical areas. Nevertheless N_w results from convective rain, as seen from Figure 4-1(b) tend to approach maritime cluster characteristics, as has happened in other instances in the same area. Therefore we understand DSDs can be highly variable even within the same location.

4.3 Uncertainties in DSD computations

Observational noise can occur in 2DVD measurements because small drops within the sample may come from different cloud regions where rain rates and microphysical processes are quite different from regions where large drops originate. The study of the microphysical processes responsible for the formation of DSDs and their evolution is an interesting but difficult subject because of the great variability of the possible processes involved. Figure 4-8 depicts the effect that the wind can cause mixing drops from different cloud regions.

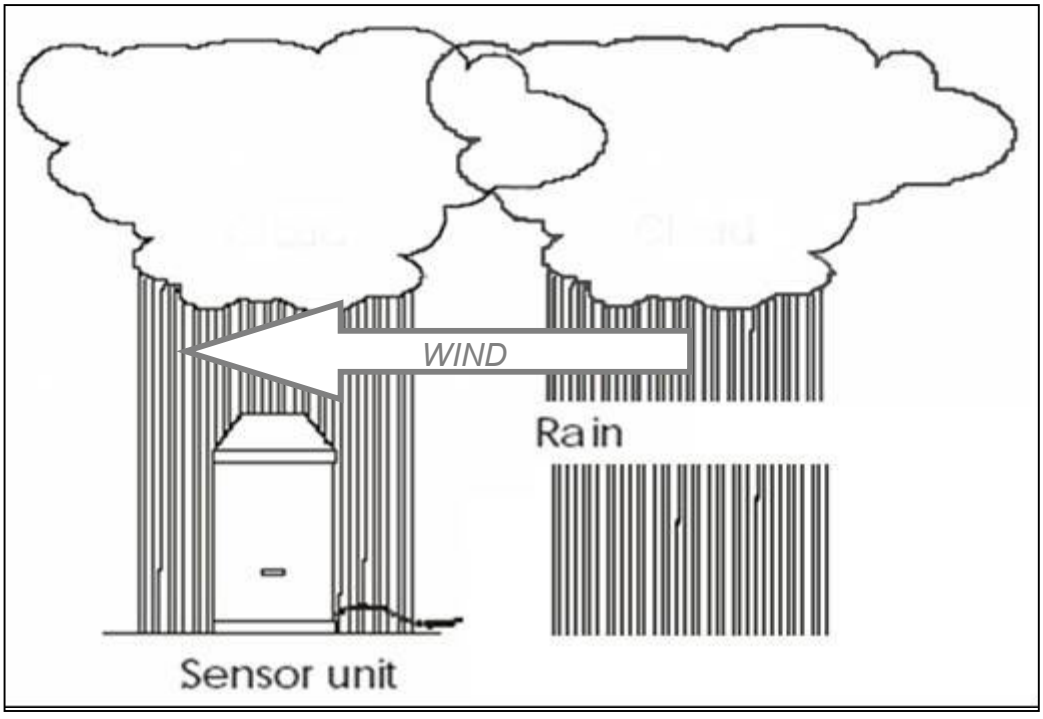

Figure 4-7 Effect of the wind in mixing drops from different cloud regions.

4.3.1 Sequential Intensity Filtering Technique (SIFT)

SIFT was developed by Lee and Zawadski to filter out observational noise concentrating on the stability of the *Z-R* relationship during a physically uniform situation.

For that purpose a record is taken of one-minute DSDs extending over several hours and average the distributions over a variable number (from one to 120) of

a) random samples (random averaging),

b) samples sequential in time (time averaging), and

c) samples sequential in either *Z* or *R* (that is, SIFT with either *R* or *Z* as the intensity parameter).

The basic steps of a SIFT procedure can be summarized as follows:

- *Z* (or *R*) is calculated for 1-min dsds for a time window
- DSDs are ordered in increasing *Z* (or *R*). A moving average of M consecutive ordered DSDs is performed to derive filtered DSDs.
- *Z* and *R* are calculated from filtered DSDs.

To investigate first efforts in applying SIFT we studied data from September 16, 2004. We used 299 continuous points and followed the steps mentioned above. Figure 4-8 illustrates a *R* vs. *Z* plot with plots before – red circles – and after –blue line – applying SIFT. It was observed that when recalculating *R* and *Z* the plot shifted up from what is was expected, as it was supposed to follow the same variations as the scatter plot. After further analysis it was found that the shifting was due the differences between the new calculated *R* and the one measured by the 2DVD and provided by FIRM_DSD program.

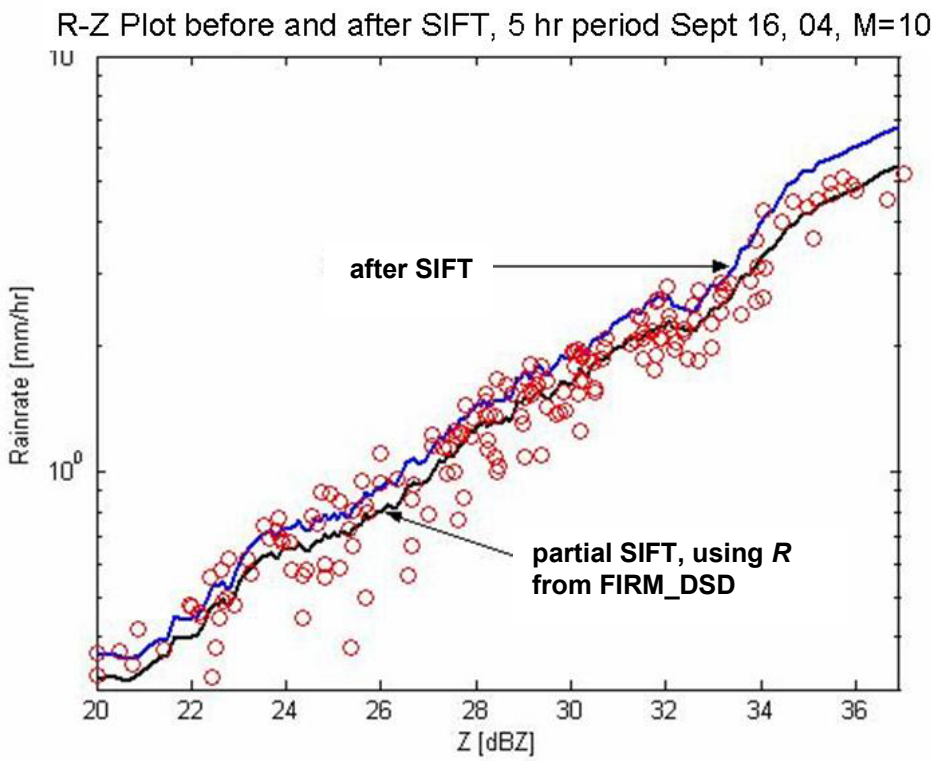

Figure 4-8 Scatter plot of *R* vs. *Z* for a five-hour period data set from September 16, 2004 (Tropical Storm Jeanne). Red circles represent *R-Z* relation before SIFT; blue line corresponds to *R-Z* afer SIFT; black line corresponds to partially applying SIFT: *R* used from FIRM_DSD (not recalculated) and *Z* recalculated as per SIFT procedure. Both lines with moving average of 10 entries (M=10).

Same figure shows also the same plot after partially applying SIFT, i.e. recalculating *Z* from reordered DSDs but using the respective *R* for each DSD provided by FIRM_DSD (black line). This line looks as a better approximation to the original data points.

In more detail Figure 4-9 include two rain rate plots that better illustrate rainfall rate differences. The blue 'o' plot shows the moving average of *R* for the respective reordered DSDs, using rain rate information provided by FIRM_DSD. On the other hand the red '+' plot shows the moving average of the recalculated *R* after reordering. It is clear here the up-shifting in rain rate values, and the explanation for the difference between the blue and black lines in Figure 4-8.

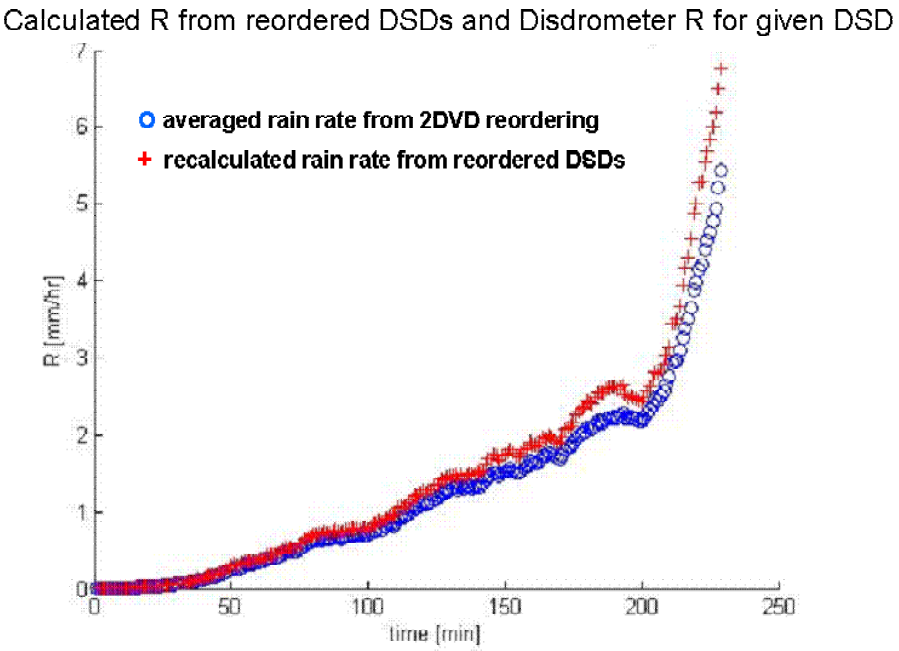

Figure 4-9 Averaged *R* from 2DVD measurements (red '+') and averaged recalculated *R* (blue 'o') after applying SIFT.

The average percent difference between the averaged 2DVD rain rate and the averaged recalculated *R* for September 16, 2004 is 12.40%. We noticed that this difference was of the order of the difference between *R* from FIRM_DSD and the calculated *R* using DSD information, that is 11.25% (see Figure 4-10). The computation of *R* using DSD information is introduced in Section 1.2; Chapter 5 presents a more detailed explanation. It might be a possibility that these two differences are related. Therefore it is our recommendation to make a deeper analysis on this subject as this shifting effect was not discussed in the work by Lee and Zawadski (2004).

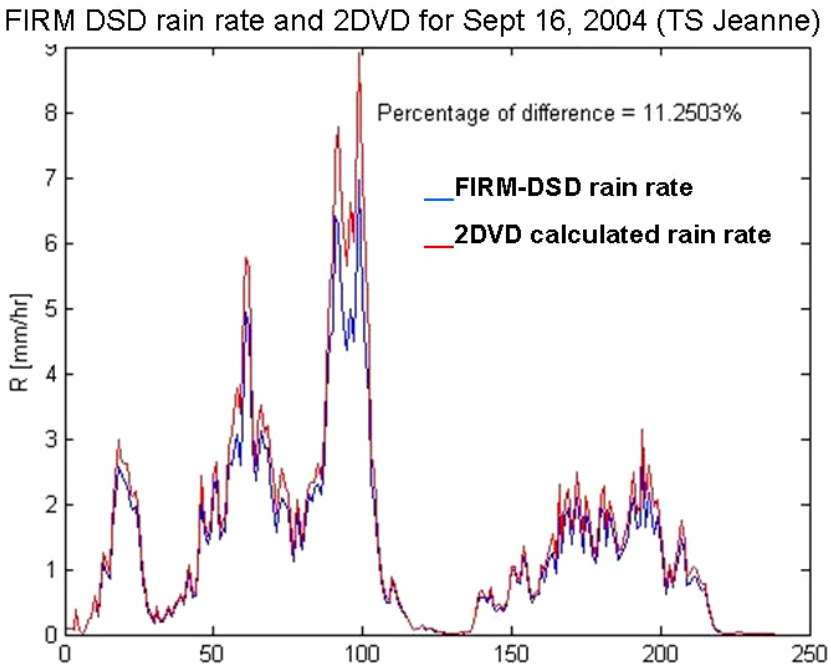

Figure 4-10 Differences between calculated (theoretical) *R* from 2DVD's DSD information (red plot) and FIRM_DSD computed *R* (blue plot).

As opposed to FIRM_DSD rainfall rate, computed *R* from theoretical equations uses velocity equations developed for stagnant air. A very detailed experiment by Kruger and Krajewski (2001) concluded the 2DVD performs well under low-wind conditions. Several issues were identified by them caused or aggravated by airflow around the instrument: 1) drop's shape deformation, 2) raindrops blown directly through the light plane slits onto the mirrors, and 3) spatial distribution distortion in the measuring area. However, the instrument described in this work is a former 2DVD, which was not a low-profile one (lower height), as the one considered in our work. Therefore some of these problems have been minimized already. Next we discuss our experiences with wind and airflow around the instrument, to continue the study on this subject as Kruger and Krajewski suggested, and to contribute with our insights.

4.3.2 Wind effects and fall velocities

Our first experience with the influence of wind on 2DVD measurements came up from a problem with the VIEW_HYD software. Tropical Storm Jeanne data produced a file slightly larger than 50 Mb. Sometimes when a file size is this big we had seen an error that did not allow us to display data with the 2DVD software. When this happened, the corresponding raw file was sent to the manufacturer, Joanneum Research, specifically to Dr. M. Schönhuber, to re-process the file and fix any data corruption. However we were able to manage such files data sets using the FIRM_DSD program. The data file from September 15, 2004 was found corrupt, so it was sent to the manufacturer as stated.

Manufacturer normally applies matching algorithms to these files, because problems could originate from mismatching particles from an area outside the virtual measuring area (refer to Figure 3-2). This treatment was done on the September 15th file and later sent back to us. While we kept working with the original file, we obtained very good results, which agreed closely with results from the ASOS rain gauge.

When we started analyzing the new file we found discrepancies of about 50% in difference with the original file. After several communications with the manufacturer, we agreed on the conclusion that strong winds affected measurements considerably. In a personal communication from Dr. M. Schönhuber (2005), he prompted the nature of the 2DVD as an area related measuring device, and that FIRM_DSD used measured velocities instead of an accepted drop diameter-velocity relationship.

We noticed that when using computed instead of measured velocities, our results agreed better with rain gauge measurements. Later we confirmed this information from Kruger and Krajewski (2001). They used three different methods to calculate *R* and when compared to rain gauge measurements they found a good agreement. Moreover, taking into account outliers on the diameter-velocity plots from VIEW_HYD for the day under study – September 15, 2004 – we were more confident with the computed velocities (see Figure 4-11). Kruger and Krajewski (2001) also discussed the outliers problem confirming, with the manufacturer's support, the hypothesis of outliers originating from particles crossing the light planes outside the measuring area.

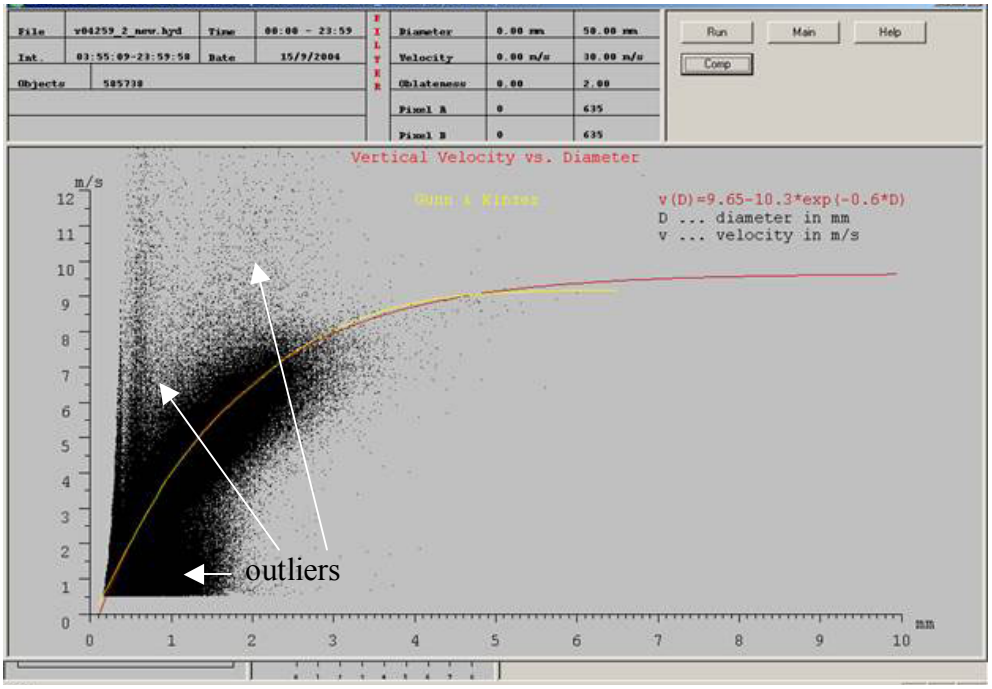

Figure 4-11 VIEW_HYD vertical velocity vs. diameter plot from September 15, 2004 showing outliers points.

Manufacturer recommended not to use the computed velocity as it derivation would be physically doubtful. In addition, he explained how to change the virtual measuring area according to the wind component, to observe the differences between FIRM_DSD computed *R*. This analysis was provided by Dr. Schönhuber as well as rainfall accumulation results, as he could manage raw data we were not able to analyze. After examining wind components for September 15th (see Figure 4-12) we noticed a strong wind component from the northeast (camera A is pointing north). Therefore it was reasonable to change the measuring area to the lower left quadrant. This is done by changing the FIRM_DSD.SET file. This file has values for lower and upper A and B cameras pixel ranges (see Figure 4-13), so one can change the virtual measuring area, normally set from 0 to 700 (700-pixel camera) for each camera. Values to change are: USE_LO_A, USE_HI_A, USE_LO_B, USE_HI_B, for respective lower A, upper A, lower B, and upper B limits.

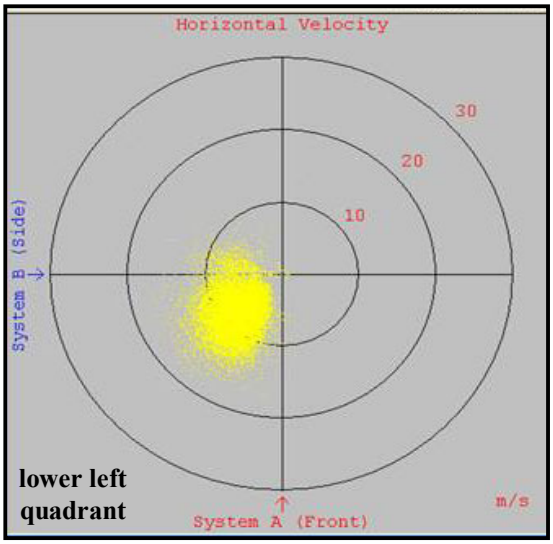

Figure 4-12 VIEW_HYD horizontal velocity plot for September 15, 2004.

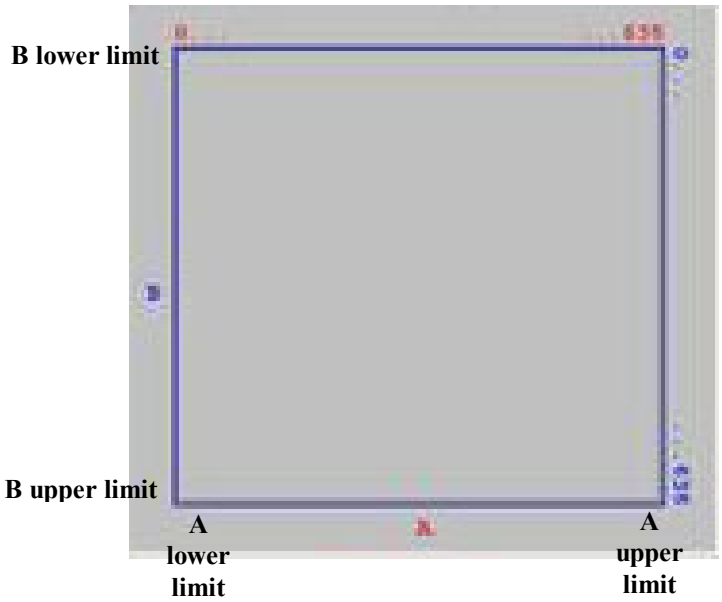

Figure 4-13 VIEW_HYD virtual measuring area.

After several changes in A and B's limits, rainfall accumulation calculations were considerably different. Results are presented in Table 4-2. Our results using computed velocity yielded 95.76 mm of accumulation for the complete day, while ASOS rain gauge measured 93.98 mm. It appears to us that applying matching algorithms is taking too many points out of the data set, resulting in significant data loss and discrepancies between 2DVD computations and other instruments.

TABLE 4-2 FIRM_DSD.SET parameter values and respective rainfall accumulation computation from modified data sets for September 15, 2004.

USE_LO_A	USE_HI_A	USE_LO_B	USE_HI_B	rainfall accumulation [mm]
0	700	0	700	49.48
0	317	318	635	65.90
0	200	435	635	68.86

When analyzing data for September 16, 2004, differences between computed accumulations using computed and measured velocities were not significantly different: 62.26 mm and 67.55 mm, respectively. ASOS rain gauge measurement for the same day was 60.21 mm, again demonstrating that measured falling velocities were still influenced by drop mismatching. By looking at Figure 4-14, it can be noticed that even when wind had a major easterly component it was not as strong as for the previous day. It is expected that stronger horizontal wind components will produce more mismatchings and induce larger errors in calculations.

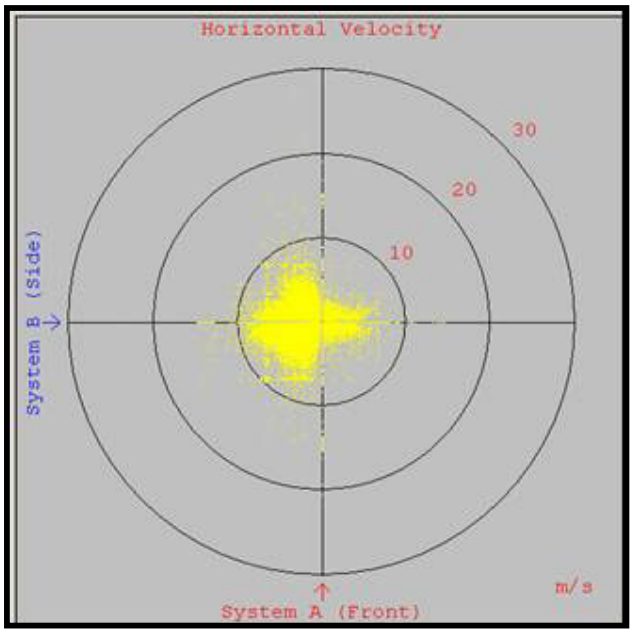

Figure 4-14 VIEW_HYD horizontal velocity plot for September 16, 2004.

Wind measurements for each day will be presented in more detail in Chapter 5, Section 5.2.

5 REFLECTIVITY COMPUTATIONS

5.1 Computations from 2DVD DSD information

Determination of proper DSDs – or *N(D)* – is crucial to calculate reflectivity *Z*. The integral form

$$Z = \int D^6 N(D) dD \tag{5.1}$$

is used for this purpose, and defines *Z* as the sixth power of the hydrometeor diameter summed over all hydrometeors in a unit volume [*Ulaby* et al., 1995]. Radars, such as National Weather Service (NWS) WSR-88D, measure *Z* and use rainfall retrieval algorithms to determine the amount of precipitation expected, hence the importance of an accurate determination of DSDs. Even if smaller drops are more numerous, calculating the sixth power of *D* causes that the fewer larger diameter drops contribute more to *Z*. In many cases DSD models overestimate the number of big drops for tropical climates, as discussed in Section 1.2 (see Figure 1-2); then the reason for rain overestimation in some cases is clearly understood. This makes it more important – to obtain detailed information about DSDs – especially for smaller diameter drops, as less weight is given to them in this calculation. An accurate number of drops will account for their appropriate contribution to *Z*.

Rainfall rate *R* and *Z* have been related through

$$Z = aR^b \tag{5.2}$$

an equation known as *Z-R* relationship. The WSR-88D precipitation processing system (PPS) converts *Z* to *R* using a *Z-R* relationship [*Vázquez*, 2001]. A list of NWS Radar Operational Center (ROC) accepted *Z-R* relationships are presented in Table 1-1 in Section 1.2. Other relationship are being suggested by former studies made in Puerto Rico, such as the one by Vázquez and Roche, but variations in rainfall characteristics made them suitable for some but not all cases.

In Puerto Rico, the Rosenfeld Tropical relationship, $Z=250R^{1.2}$, is widely used, though lately it has been changed for certain events, following local NWS findings from their research.

With the intention of comparing and determining *Z-R* relationships, new *R*s are calculated from 2DVD DSD information. To calculate *R* the following equation was used from Bringi and Chandrasekar (2001).

$$R = 0.6\pi \times 10^{-3} \int D^3 v(D) N(D) dD \qquad (5.3)$$

This equation yields *R* in mm*hr^{-1} when *D* is in mm, *v(D)* is in m*s^{-1}, and *N(D)dD* is in drops*m^{-3}. Drop terminal velocity *v(D)* was found from same work (*Bringi* and *Chandrasekar*, 2001).

$$v(D) = 9.65 - 10.3e^{(-0.6D)} \qquad (5.4)$$

After calculating *Z* and *R* using (5.1) and (5.3), respectively, it is necessary to determine *Z-R* relationships between them, fitting data to find coefficients *a* and *b* that optimally fulfills equation (4). Base 10 logarithms were found on each side of (5.2) to make lineal instead of power or exponential fitting. Table 5-2 presents the summary of results from the coefficients found on each day for different *Z-R* relationships. It also shows the differences caused by

differences in R between using FIRM_DSD data and calculating R using (5). Since FIRM_DSD uses measured fall velocities instead of (5.4), results account for that difference.

TABLE 5-1 Summary of results for a and b coefficients found for Z-R relationships.

TS Jeanne	15 Sep 2004	16 Sep 2004
Using calculated R from 2DVD-measured DSDs	$Z = 228.89\ R^{1.24}$	$Z = 428.35\ R^{1.29}$
Using R from FIRM_DSD	$Z = 414.4\ R^{1.38}$	$Z = 523.26\ R^{1.32}$
Rainfall characterization	Mostly stratiform, some convective 349 stratiform, 137 convective Total: 608 continuous data points (10.13 hrs).	Mostly stratiform 156 stratiform, 1 convective Total: 239 continuous data points (3.98 hrs).
Known Z-R relationships	Rosenfeld tropical $Z = 250\ R^{1.2}$ Convective $Z = 300\ R^{1.4}$	Tropical Maritime $Z = 335\ R^{1.37*}$ Thunderstorms $Z = 450\ R^{1.46**}$
		*Tokay et al., 1995 **Fujiware, 1965

5.2 Comparisons to NEXRAD measured reflectivity

NWS provided us with reflectivity data from NEXRAD for the two days of the storm, September 15 and 16, 2004. Only data available was in 5 dBZ increments and 5 minutes time resolution. It was expected that the poor resolution of the data, compared to data computed from 2DVD's DSDs, will yield significant differences. Figure 5-2 shows reflectivity vs. time plots for both days of the event, after both plots were matched in time for minimum difference.

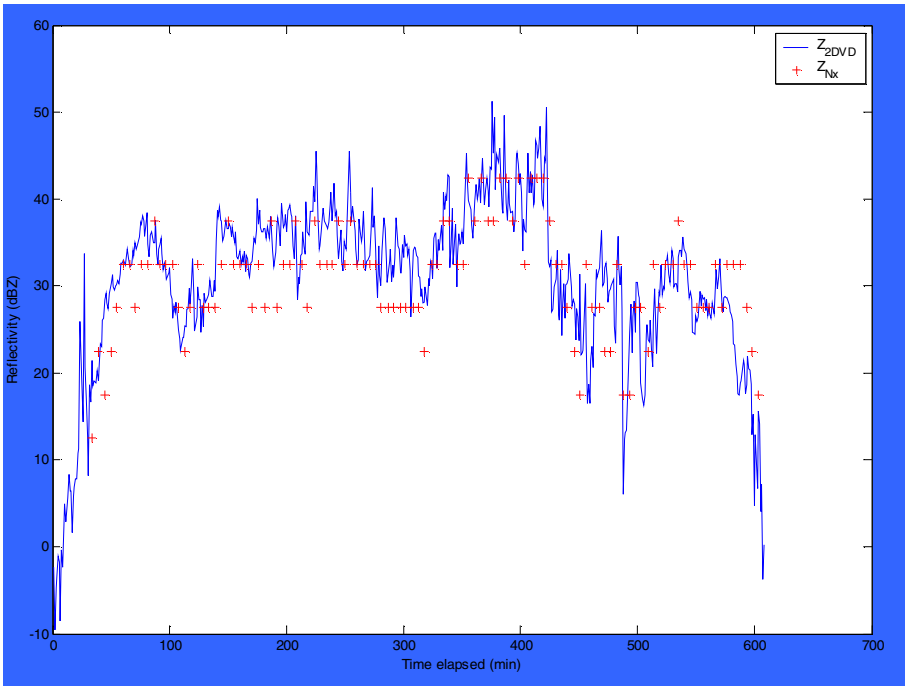

(a)

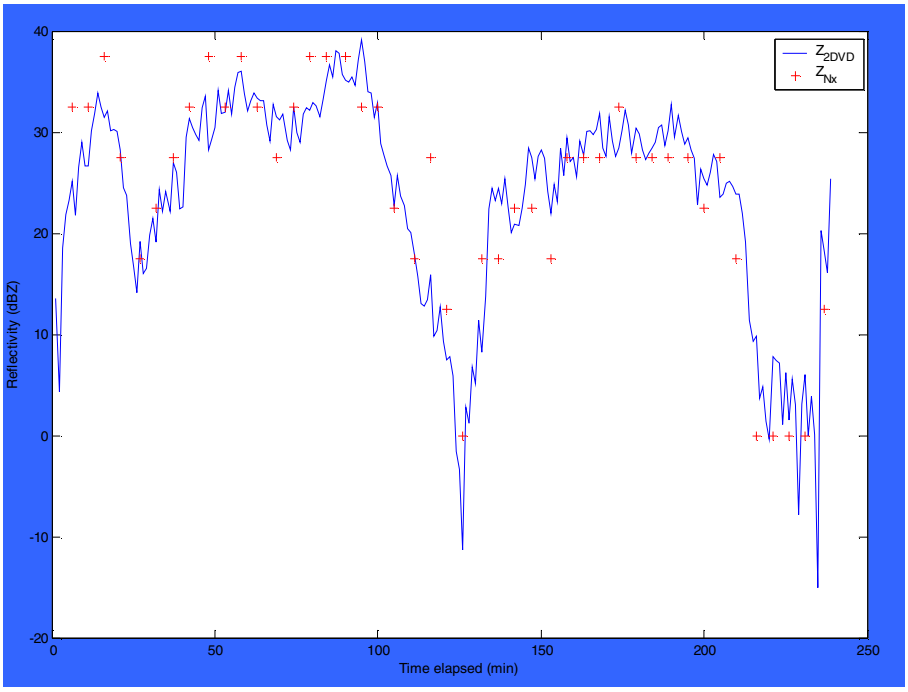

(b)

Figure 5-1 Comparison between NEXRAD measured *Z* (red +) and *Z* (blue plot) computed from 2DVD measured DSDs: (a) September 15th, and (b) September 16th, 2004.

Above the NWS premises, NEXRAD collects measurements at approximately 4,000 feet, or 1,219.5 meters. Therefore it is expected that there is a time lag of measurements by 2DVD of drops coming from the same region NEXRAD is measuring. We calculated the difference between the *Z* values from both instruments and determine from these numbers which was the shifting in time needed to match both measurements, identifying the time where maximum differences were the lowest on that time period. Shifting times required for matching plots are presented in Table 5-2 along with average winds for each day. Figures 4-12 and 4-14 in Section 4.3.2, illustrate the direction of wind displayed by the higher concentration of drops towards to the wind direction.

TABLE 5-2 Shifting time to match *Z* plots and corresponding average horizontal wind.

Day	Time difference to match both *Z*s (minutes)	Average horizontal wind (m/s)
September 15, 2004	2	6.8 NE
September 16, 2004	4	2.7 E

As seen here, from Table 5-3 where comparison results are shown, even when fewer data points are available for comparison, differences in *Z* from September 16th are lower than for the 15th. A factor that might explain these discrepancies is the wind speed, which in this storm reached 31.5 m/s maximum for September 15th and much calmed –7.5 m/s maximum – for the 16th. These winds had a strong northeast component on the first day of the storm and a strong east component on the second; together with vertical winds – data that is not available for this

study – add to the falling time of drops, accounting for the time shifting between measurements. These factors make more difficult the possibility of matching both quantities.

Even though bigger differences were expected in the results, Table 5-4 demonstrates that measurements for this event matched quite well. Percent difference calculated yield less than 1% and 3%, respectively for the 15th and 16th of September. Therefore it takes us to asses expected rain accumulation calculations for both days, to verify if they match as well.

TABLE 5-3 Differences between reflectivity measured by NEXRAD (Z_{Nx}) and reflectivity computed using 2DVD measured DSDs (Z_{2DVD}) for the time period shown in Figure 5-2. Calculations were performed after best match of graphs.

Comparison results (dBZ)	September 15th	September 16th
max diff	13.8982	11.6318
min diff	0.0052	0.0388
avg Z_{Nx}	30.8945	24.2222
avg Z_{2DVD}	30.7486	23.6475
Percent difference	0.47%	2.4%

Uncertainties discussed in Chapter 3, Section 3.3, introduces inconsistencies in measurements that could cause 2DVD to measure drops coming from a cloud region different than the one NEXRAD is taking measurements. This shows in the results presented here regarding the differences in *Z*, though given the poor resolution of NEXRAD data provided by NWS (5 dBZ range for each measurement), *Z* comparisons outcomes were better than expected.

Furthermore, time resolution of NEXRAD measurements is 5 minutes and 2DVD's is one minute, adding to the difficulty of comparing both.

6 CONCLUSIONS AND FUTURE WORK

Fundamentally, at least two different types of DSDs are involved in Puerto Rico's rainfall systems. This validates findings by Ulbrich, Petitididier, and Campos (1999) that DSDs are highly variable between coastal and mountainous zones, even for a small region as the island of Puerto Rico, which posses a very complex orography. The importance of considering variations of *Z-R* relationships between ocean and land surfaces, as proposed by Ulbrich et al. (1999), is therefore preliminary confirmed. This work contributes with supplementary data analysis for tropical environments that has been understood as necessary.

Even for the same area we obtained two different *Z-R* relationships that could cause an over – or under – estimation of about 80% in rain rate values. It is suggested to check with NWS San Juan WFO to verify if indeed rainfall estimates for this storm were under or overestimated. We will present our findings and dialogue alternatives to further investigate our results.

More events will be required to validate rainfall types differences found in this work. It was expected to find a bigger convective component in a tropical storm event, so further analysis of events with considerable amount of precipitation is suggested. It is recommended as well to use other methods to separate between stratiform and convective rain. Other methods use reflectivity values and/or reflectivity vertical images to identify stratiform or convective events. We have been told that events in our region are localized and therefore are convective by nature. Our recommendation comes from the examination of histograms of D_m and $\log_{10}\langle N_w \rangle$, where we

observed a small additional component of other values besides the mean and mode values (see Figures 4-5 and 4-6).

Differences in measured and computed fall velocities caused differences in *Z-R* relationships when using FIRM_DSD rain rate output and calculated *R* from measured DSDs. These differences were higher when stronger horizontal wind components are present. Our study was based on a tropical storm event where strong winds are known, then other rain events with lower wind velocities should be considered to validate the DSD characterization. It is necessary to compare both results with rain gauge or other validated data as well as with NEXRAD data, to decide what would be the best path to follow when computing expected *Z*. For that reason 2DVD literature specifies that it provides accurate data under low-wind conditions.

As future work, additional significant rainfall data from other events is available; these could be used to compare and validate these results. Data from other tropical regions can be considered and used for comparison purposes.

In terms of *Z*, some low-resolution data (3-minutes, 5 dBZ intervals) has been obtained from NWS local weather forecast office, and even when it will not serve for exact comparisons, it will impart confidence in our results.

Finally, existing techniques to filter errors that can be introduced by drops coming from different regions of the clouds are being analyzed. As bigger drops have different fall velocities than smaller drops, DSD estimation on the ground could not be in accordance with what radars are measuring above, causing errors in DSDs and therefore in *Z* computations. These errors are considered as observational noise. One of these techniques is the Sequential Intensity Filtering Technique (SIFT) which concentrates on the stability of the *Z-R* relationship during a physically

uniform situation [*Schönhuber*, 2000]. It is recommended that SIFT, aimed to filter out observational noise, be further investigated, applying it to data sets considered here and to future sets as they become available from this ongoing measurement experiment.

How great is God—beyond our understanding! The number of his years is past finding out. "He draws up the drops of water, which distill as rain to the streams; the clouds pour down their moisture and abundant showers fall on mankind. Who can understand how he spreads out the clouds, how he thunders from his pavilion? Job 36:26-29 (New International Version)

REFERENCES

Automated Surface Observing System (ASOS) description [Online]. Available from http://www.nws.noaa.gov/ost/asostech.html, 1999.

Aydin, K., and S.E. A Daisley, "Relationships Between Rainfall Rate and 35 GHz Attenuation and Differential Attenuation: Modeling the Effects of Raindrop Size Distribution, Canting, and Oscillation," *IEEE Transactions on Geoscience and Remote Sensing*, Vol. 40, No. 11, November 2002.

Bennett, S., V. Grusbisic, and R.M. Rasmussen, "Gravity Waves, Rainbands, and Deep Convection Induced by Trade Wind Flow Past Puerto Rico." Available from http://www.srh.noaa.gov/sju/tradewindpaper.html .

Bringi, V.N., and V. Chandrasekar, Polarimetric Doppler Radar, First edition, 2001.

Bringi, V.N., T.D. Keenan, and V. Chandrasekar, "Correcting C-Band Radar Reflectivity and Differential Reflectivity Data for Rain Attenuation: A Self-Consistent Method With Constraints," *IEEE Transactions on Geoscience and Remote Sensing*, Vol. 39, No. 9, September 2001.

Carter, M., J.B. Elsner, and S. Bennett, "Monthly Rainfall Climatology for Puerto Rico," *Southern Topics* (National Weather Service Southern Region Headquarters publication), 1997. Available from http://www.srh.noaa.gov/topics/attach/html/ssd97-40.htm.

Collaborative Adaptive Sensing of the Atmosphere (CASA) Engineering Research Center, "Overview" [Online]. Available from http://www.casa.umass.edu, 2003.

Denby, B., P. Golé, and J. Tarniewicz, "Structured Neural Network Approach for Measuring Raindrop Sizes and Velocities," *IEEE Signal Processing Society Workshop on Neural Networks for Signal Processing*, 1998.

Donovan, B. et al., "A DCAS Network for QPE on the Island of Puerto Rico," *American Institute of Aeronautics and Astronautics*, 2004.

Doviak, R. J.and D. S. Zrnic, Doppler Radar and Weather Observations, Second edition, Academic Press, San Diego, 1993.

Förster, J., "Rain Measurement on Buoys Using Hydrophones," *IEEE Journal of Oceanic Engineering*, Vol. 19, No. 1, January 1994.

IDL information page [Online]. Available from http://www.rsinc.com/idl/.

Joss, J. and A. Waldvogel, "Raindrop size distribution and sampling errors," *Journal of Atmospheric Sciences*, Vol. 26, pp. 566-569, 1967.

Kafando, P., and M. Petitdidier, "An attempt to calibrate the UHF strato-tropospheric radar at Arecibo using NEXRAD and disdrometer data," *MST10 Workshop, CETP/CNRS*, Velizy, France, 2003.

Kruger, A., W.F. Krajewski, "Two-Dimensional Video Disdrometer: A description," *Journal of Atmospheric and Oceanic Technology*, Vol. 19, pp. 602-617, 2001

Lee, GyuWon, and I. Zawadzki, "Erros in Rain Measurement by Radar due to the Variability of Drop Size Distributions," *Sixth International Symposium on Hydrological Applications of Weather Radar*, Melbourne, Australia, 2-4 February 2004.

Meneghini, R. et al., "Differential-frequency Doppler weather radar: Theory and experiment," *Radio Science*, Vol. 38, No. 3, February 2003.

RealVNC (Virtual Network Computing) page [Online]. Available from http://www.realvnc.com/, 2002.

Rincón, R.F. et al. "Estimation of Path-Average Rain Drop Size Distribution using the NASA/TRMM Microwave Link," *IEEE International Geoscience and Remote Sensing Symposium (IGARSS)*, Vol. 3, 9-13 July, 2001.

Rincón, R.F. and R. Lang, "Microwave Link Dual-Wavelength Measurements of Path-Average Attenuation for the Estimation of Drop Size Distribution and Rainfall," *IEEE Transactions Geoscience and Remote Sensing*, Vol. 40, No. 4, pp.760-770, April 2002.

Schönhuber, M. et al., "Weather Radar versus 2D-Video-Distrometer Data," *Proceedings of the III International Symposium on Hydrological Applications of Weather Radars*, São Paulo, Brazil, August 20-23, 1995.

Schönhuber, M., H.E.Urban, J.P.V.Poiares Baptista, W.L.Randeu, and W.Riedler. "Measurements of Precipitation Characteristics by a New Distrometer," Institute for Applied Systems Technology, JOANNEUM RESEARCH, Graz/Austria, 1994.

Schönhuber, M., "Distrometer results obtained in various climates and their application to weather radar data inversion," *ESA SP-444 Proceedings, Millennium Conference on Antennas & Propagation*, Davos, Switzerland, April 9-14, 2000.

Simpson, J., C. Kummerow, W.-K. Tao, and R. F. Adler, "On the Tropical Rainfall Measuring Mission (TRMM)," *Meteor. Atmos. Phys*., vol. 60, pp. 19-36, 1996.

Takahashi, N.; H. Uyeda, Y. Asuma, S. Shimizu, Y. Fujiyoshi, S. Sato, T. Endoh, K. Takeuchi, R. Shirooka and A. Sumi, "Radar observations of tropical clouds on the Manus Island, Papua New Guinea," *Geoscience and Remote Sensing Symposium,. IGARSS '93. Better Understanding of Earth Environment., International,* vol.2, pp. 615 –617, 1993

Ulaby, F. T., R. K. Moore and A. K. Fung, Microwave Remote Sensing: Active and Passive, Vol. 1, Artech House, Norwood, 1981.

Ulbrich, C. W., "Natural variations in the analytical form of the raindrop size distribution," *J. Climate Appl. Meteor.,* vol. 22, pp. 1764-1775, 1983.

Ulbrich, C. and N.E. Miller, "Experimental Test of the Effects of Z-R Law Variations on Comparison of WSR-88D Rainfall Amounts with Surface Rain Gauge and Disdrometer Data", *Weather and Forecasting*, Vol. 16, pp. 369-374, American Meteorological Society, June 2001.

Ulbrich, C. W., M. Petitididier, and E.F. Campos, "Radar Properties of Tropical Rain Found from Disdrometer Data at Arecibo, P.R.," Reprinted from the preprint volume of the *29th International Conference on Radar Meteorology*, July 12-16, 1999, Montreal, Quebec, Canada, by the American Meteorological Society Society, Boston, Massachusetts, 1999.

Ulbrich, C. W., L. G. Lee, "Rainfall Measurement Error by WSR-88D Radars due to Variations in Z–R Law Parameters and the Radar Constant," *Journal of Atmospheric and Oceanic Technology*, American Meteorological Society, August 1999.

Vázquez, M. and A. Roche, "An evaluation of WSR-88D rainfall estimates across Puerto Rico during Hurricane Debbie," Internal Document from NWS San Juan Weather Forecast Office, Carolina, Puerto Rico.

APPENDIX A. MATLAB CODES

%%%Program to find continuous data, calculate DSD parameters, apply SIFT technique and plot results

```
clc
clear all
dsd=xlsread('v04260_1.xls'); %to read Microsoft Excel file with dsd values

% diameters values in [mm]; as they don't change they are defined here
% instead of reading them from file
D=[0.125:0.25:10.125];

%amounts of minutes in original file; every minute has 41 dsd values for 41
%different diameters
minutes=(length(dsd)-1)/42;
skip=0; %variable needed to jump to next dsd value for the same diameter,
      %as same diameter is every 41 minutes

%rearrange dsd per minute in a single matrix with rows corresponding min1,
%min2, min3... and every column represents the d1, d2, d3,....

for i=1:minutes
   for j=1:41
      if dsd(i+j+skip,9)>=0 %fixing problem with Excel giving zeros as NaN
        dsd_per_min(i,j)=dsd(i+j+skip,9); %important to notice column number
                                  %for dsd values; in this case
                                  %is '9'.
      else
         dsd_per_min(i,j)=0;
      end
   end
   rainrate(i)=dsd(i+j+skip+1,2); %important to notice column number for rainrate
                          %values; in this case is '3' for 15Sep (file v04259_2.xls)
                          %and '2' for 16Sep (file v04260_1.xls)
   ZNx(i)=dsd(i+j+skip+1,6);
   time(i)=dsd(i+j+skip-1,1); %acquiring time to check for continuous data
   skip=skip+j;
end

%Next steps are for determining sets of continuos data and taking the set
%with more continuous data points
time=time./0.00069444;
diff_time=diff(time);
ind_discont=find(diff_time > 1.5); %look for indexes when time differences are greater than one minute;
                        %needed to use > 1.5 because differences are
                        %not exactly 1.0.
diff_idisc=diff(ind_discont);
[max_diff,max_diff_index]=max(diff_idisc); %look for max. difference between indexes of discontinuities;
                                  %as more distance there is between differences more
                                  %continuous minutes will be between them
longest_cont_ind(1:2)=ind_discont(max_diff_index:max_diff_index+1);
```

```
cont_ind=[(longest_cont_ind(1)+1) longest_cont_ind(2)];

% creating new dsd matrix with continuous data from dsd_per_min
new_ind=1;
for i=cont_ind(1):cont_ind(2)
   dsd_cont(new_ind,:)=dsd_per_min(i,:);
   R_cont(new_ind)=rainrate(i);
   ZNx_cont(new_ind)=ZNx(i);
   new_ind=new_ind+1;
end

D6=D.^6;
D4=D.^4;
D3=D.^3;

for n=1:length(dsd_cont)
   %calculating moments dD=0.25 mm
   dm_6(n,:)=(dsd_cont(n,:).*D6.*0.25);
   dm_4(n,:)=(dsd_cont(n,:).*D4.*0.25);
   dm_3(n,:)=(dsd_cont(n,:).*D3.*0.25);
   %calculating rain rate from 2dvd dsd info to compare with FIRM_DSD
   %output
   rainrate_2dvd(n)=sum(dsd_cont(n,:).*D3.*0.25.*(9.65-10.3*exp(-0.6.*D)));
end

%adding rows of fourth moment and third moment to calculate sum for each
%minute; need to transverse matrix to sum rows instead of columns
sumdm_4=sum(dm_4');
sumdm_3=sum(dm_3');

%calculating dsd characterizations and Z
Dm_avg= sumdm_4./sumdm_3;

W_avg=sumdm_3.*pi*.001/6;
N_avg=(W_avg./(Dm_avg.^4))*81.487E03;

Z_numeric=sum(dm_6');
%calculating standard deviation of average rainrate
for n=1:length(R_cont)-5
   std_R(n)=std(R_cont(n:n+4));
   if (std_R(n)<= 1.5 & R_cont(n) >= 0.5)
      test_strat(n)=n;
   elseif (std_R(n) > 1.5 & R_cont(n) >= 5)
      test_conv(n)=n;
   end
end

% %calculating index of rainrate to separate stratiform from convective rain
% %stratiform: R >= 0.1 mm/hr
iR_strat=nonzeros(test_strat);
R_strat=R_cont(iR_strat);
%calculating index of rainrate to separate stratiform from convective rain
```

```
%convective: R > 5 mm/hr
iR_conv=nonzeros(test_conv);
R_conv=R_cont(iR_conv);

%changing numeric Z to dBZ
Z=10.*(log10(sum(dm_6')));

%shifting Z
Z_shift=[Z(5:end) Z(1) Z(2) Z(3) Z(4)];
ZNx_shift=[ZNx_cont(1:end)];
Z_dif=abs(Z_shift-ZNx_shift);
Z_dif_pct=Z_dif./(abs((Z_shift+ZNx_shift))./2)*100;
maxZ_difpct=max(Z_dif_pct)
maxZ_dif=max(Z_dif)
ZNx_nonan=ZNx_cont(~isnan(ZNx_cont));
ZNx_avg=mean(ZNx_nonan)
Z_mean=mean(Z)
%ZNx_cont(isnan(ZNx_cont))=[0];

%sorting Z in ascending order but keeping original indexes
[Z_sort,orig_Zind]=sort(Z);

%using original indexes to match dsds and rainrate
for i=1:max(orig_Zind)
   dsd_sort(i,:)=dsd_cont(orig_Zind(i),:);
   R_sort(i,:)=R_cont(orig_Zind(i));
end

%averaging size M for SIFT
M=10;
   for n=1:length(dsd_sort)-M
      dsd_avg(n,:)=mean(dsd_sort(n:n+M,:));
      R_avg(n)=mean(R_sort(n:n+M));
   end
%
%recalculating moments to recalculate Z
    for n=1:length(dsd_avg)
       dmavg_6(n,:)=(dsd_avg(n,:).*D6.*0.25);
       dmavg_4(n,:)=(dsd_avg(n,:).*D4.*0.25);
       dmavg_3(n,:)=(dsd_avg(n,:).*D3.*0.25);
       rainrate_avg(n,:)=(dsd_avg(n,:).*D3.*0.25.*(9.65-10.3*exp(-0.6.*D)));
    end

%recalculating sum of moments
sumdmavg_4=sum(dmavg_4');
sumdmavg_3=sum(dmavg_3');
%recalculating rainrate with new dsds
R_avg_calc=0.6*pi*1e-3*(sum(rainrate_avg'));
R_2dvd=0.6*pi*1e-3*(rainrate_2dvd);

%recalculating dsd characterizations and (Z)
Dmsort_avg= sumdmavg_4./sumdmavg_3;
```

```
Wsort_avg=sumdmavg_3.*pi*.001/6;
Nsort_avg=(Wsort_avg./(Dmsort_avg.^4))*81.487E03;

Z_num=sum(dmavg_6');
Z_avg=10.*(log10(Z_num));

%percentage of difference between R calculated from 2dvd dsd info and R
%calculated by FIRM_DSD
diff_pcnt=((R_2dvd-R_cont)./((R_2dvd+R_cont)/2))*100;
diff_pcnt_avg=mean(diff_pcnt);


%curve fitting functions to find Z-R relationship

p = polyfit(log10(Z_num),log10(R_avg_calc),1);%after SIFT
b = 1/p(1)
a = 10^(-1*p(2)*b)
f = polyval(p, Z_num);
plot(Z_num,R_avg_calc,'LineWidth',2)
hold on
semilogy(log10(Z_num),f,'-')
% plot(log10(Z_num),log10(f),'-')
hold off

%plot
semilogy(Z_avg,R_avg_calc,'LineWidth',2)
title(['R-Z Scatter plot before and after SIFT, 4-hr period on 16Sep2004 - M = ',num2str(M)])
ylabel('Rainrate [mm/hr]')
ylim([0.3 10])
xlabel('Z [dBZ]')
xlim([20 max(Z_avg)])
hold on
semilogy(Z_avg,R_avg,'k','LineWidth',2)
scatter(Z,R_cont,'r')
hold off
%
figure(2)
time=[1:1:length(R_avg)];
scatter(time,R_avg)
xlabel('time [min]')
ylabel('R [mm/hr]')
hold on
scatter(time,R_avg_calc,'+','r')
title('Calculated R from reordered dsds and disdrometer R for given dsd')
hold off
%
% %plots of calcualted R from 2dvd data (R_2dvd) and calculated R from
% %FIRM_DSD (R_cont)
figure(3)
plot(R_cont)
title('FIRM-DSD rain rate (blue) and 2dvd rain rate (red) - 15sep2004')
ylabel('R [mm/hr]')
```

```
text(105,8,['Percentage of difference = ',num2str(diff_pcnt_avg),'%'])

hold on
plot(R_2dvd,'r')
hold off

%plots of NEXRAD reflectivity Z and computed Z from DSD info
figure(3)
plot(Z_shift)
hold on
plot(ZNx_shift,'r+')
hold off
```

%%%Program to classify convective data, calculate DSD parameters, and plot results

```
clc
clear all
dsd1=xlsread('V04259_2.xls');

D=[0.25:0.25:10.25];

minutes1=(length(dsd1)-1)/42;
skip=0;

%rearrange dsd per minute in a single matrix with rows corresponding min1,
%min2, min3... and every column represents the d1, d2, d3,....

for i=1:minutes1

    for j=1:41
       if dsd1(i+j+skip,9)>=0 %fixing problem with Excel giving zeros as NaN
         dsd_per_min1(i,j)=dsd1(i+j+skip,9);
       else
          dsd_per_min1(i,j)=0;
       end
   end
   rainrate1(i)=dsd1(i+j+skip+1,3);
   skip=skip+j;
end

% dsd2=xlsread('v04260_1.xls');
minutes2=(length(dsd2)-1)/42;
skip=0;

for i=1:minutes2
   for j=1:41
       if dsd2(i+j+skip,9)>=0 %fixing problem with Excel giving zeros as NaN
         dsd_per_min2(i,j)=dsd2(i+j+skip,9);
       else
          dsd_per_min2(i,j)=0;
```

```
        end
    end
    rainrate2(i)=dsd2(i+j+skip+1,2);
    time2(i)=dsd2(i+j+skip-1,1); %acquiring time to check for continuos data
    skip=skip+j;
end

dsd_per_min=[dsd_per_min1;dsd_per_min2];
rainrate=[rainrate1(1:end) rainrate2(1:end)];
%time=[time1(1:end) time2(1:end)];


D6=D.^6;
D4=D.^4;
D3=D.^3;

for m=1:2:length(dsd_per_min)-1
    n=(m-1)/2+1;
        dsd_avg(n,:)=(dsd_per_min(m,:)+dsd_per_min(m+1,:))/2;
        dm_6(n,:)=(dsd_per_min(n,:).*D6.*0.25);
        dm_4(n,:)=(dsd_per_min(n,:).*D4.*0.25);
        dm_3(n,:)=(dsd_per_min(n,:).*D3.*0.25);
        rainrate_avg(n)=(rainrate(m)+rainrate(m+1))/2;
end

%calculating standard deviation of average rainrate
for n=1:length(rainrate_avg)-5
    std_R(n)=std(rainrate_avg(n:n+4));
    if (std_R(n)>1.5 & rainrate_avg(n)>=5)
        test_conv(n)=n;
    end
end

%calculating index of rainrate to separate stratiform from convective rain
%convective: R > 5 mm/hr
iR_conv=nonzeros(test_conv);
R_conv=rainrate_avg(iR_conv);

%adding rows of dsd*D^4 and dsd*D^3 to calculate sum for each minute
sumdm_4=sum(dm_4');
sumdm_3=sum(dm_3');
Dm_avg= sumdm_4./sumdm_3;

W_avg=sumdm_3.*pi*.001/6;
N_avg=(W_avg./(Dm_avg.^4))*81.487E03;

Z_num=sum(dm_6');

%selecting Dm, Nw and Z for respective stratiform and convective rain using
%indexes determined above
Dm_avg_conv=Dm_avg(iR_conv);
avgDmc=mean(Dm_avg_conv) %avg Dm for stratiform rain
```

```
std_Dmc=std(Dm_avg_conv) %standard deviation of Dm for stratiform rain

Nw_conv=N_avg(iR_conv);
avgNwc=mean(Nw_conv);
std_Nwc=std(Nw_conv);
avg_logNw=log10(avgNwc)
std_logNw=std(log10(Nw_conv))
log10(std_Nwc);

Z_conv=Z_num(iR_conv);
Z=10.*(log10(Z_conv));

%determining R-Z relationship
p = polyfit(log10(Z_conv),log10(R_conv),1);
b = 1/p(1)
a = 10^(-1*p(2)*b)

figure(1)
scatter(Dm_avg_conv,log10(Nw_conv),'x');
title('Nw vs. Dm for TS Jeanne - convective rain');
xlabel('Dm [mm]');
ylabel('log10(Nw) [mm^-1 * m^-3]');
%

figure(2)
scatter(R_conv,Dm_avg_conv,'x');
title('Dm vs. rainrate for TS Jeanne - convective rain');
xlabel('Rainrate [mm/hr]');
ylabel('Dm [mm]');
%
figure(3)
scatter(R_conv,log10(Nw_conv),'x');
title('Nw vs. rainrate for TS Jeanne - convective rain');
xlabel('Rainrate [mm/hr]');
ylabel('log10(Nw) [mm^-1 * m^-3]');
%
figure(4)
hist(Dm_avg_conv,20);
title('Histogram of Dm for TS Jeanne - convective rain');
%
figure(5)
hist(log10(Nw_conv),20);
title('Histogram of log10(Nw) for TS Jeanne - conv rain');
%
figure(6)
plot(Z);
title('Reflectivity for TS Jeanne - convective rain');
ylabel('Z [dBZ]');



%%%Program to classify stratiform data, calculate DSD parameters, and plot results
```

```
clc
clear all
dsd1=xlsread('v04259_2.xls');

D=[0.125:0.25:10.125];

minutes1=(length(dsd1)-1)/42;
skip=0;

%rearrange dsd per minute in a single matrix with rows corresponding min1,
%min2, min3... and every column represents the d1, d2, d3,....
for i=1:minutes1
   for j=1:41
      if dsd1(i+j+skip,9)>=0 %fixing problem with Excel giving zeros as NaN
        dsd_per_min1(i,j)=dsd1(i+j+skip,9);
      else
         dsd_per_min1(i,j)=0;
      end
   end
   rainrate1(i)=dsd1(i+j+skip+1,3);
   time1(i)=dsd1(i+j+skip-1,1); %acquiring time to check for continuos data
   skip=skip+j;
end

% dsd2=xlsread('v04260_1.xls');
minutes2=(length(dsd2)-1)/42;
skip=0;

for i=1:minutes2
   for j=1:41
      if dsd2(i+j+skip,9)>=0 %fixing problem with Excel giving zeros as NaN
        dsd_per_min2(i,j)=dsd2(i+j+skip,9);
      else
         dsd_per_min2(i,j)=0;
      end
   end
   rainrate2(i)=dsd2(i+j+skip+1,2);
   time2(i)=dsd2(i+j+skip-1,1); %acquiring time to check for continuos data
   skip=skip+j;
end

dsd_per_min=[dsd_per_min1;dsd_per_min2];
rainrate=[rainrate1(1:end) rainrate2(1:end)];
time=[time1(1:end) time2(1:end)];


D6=D.^6;
D4=D.^4;
D3=D.^3;

for m=1:2:length(dsd_per_min)-1
```

```
   n=(m-1)/2+1;
      dsd_avg(n,:)=(dsd_per_min(m,:)+dsd_per_min(m+1,:))/2;
      dm_6(n,:)=(dsd_per_min(n,:).*D6.*0.25);
      dm_4(n,:)=(dsd_per_min(n,:).*D4.*0.25);
      dm_3(n,:)=(dsd_per_min(n,:).*D3.*0.25);
      rainrate_avg(n)=(rainrate(m)+rainrate(m+1))/2;
      rainrate_avg_calc(n)=sum(dsd_avg(n,:).*D3.*0.25.*(9.65-10.3*exp(-0.6.*D)));
end
%
R_avg_calc=0.6*pi*1e-3*(rainrate_avg_calc);
accumASOS_16sep=[0.01 0 0 0 0.01 0 0 0 0.1 0.26 0.43 0.19 0.93 0.76 0.1 0.15 0.03 0 0 0.07 0.51 0.11
0.04 0];

%calculating standard deviation of average rainrate
for n=1:length(rainrate_avg)-5
   std_R(n)=std(rainrate_avg(n:n+4));
   if (std_R(n)<= 1.5 & rainrate_avg(n) >= 0.5)
      test_strat(n)=n;
   end
end

% %calculating index of rainrate to separate stratiform from convective rain
% %stratiform: R >= 0.1 mm/hr

iR_strat=nonzeros(test_strat);
R_strat=rainrate_avg(iR_strat);

%adding rows of dsd*D^4 and dsd*D^3 to calculate sum for each minute
sumdm_4=sum(dm_4');
sumdm_3=sum(dm_3');

Dm_avg= sumdm_4./sumdm_3;

W_avg=sumdm_3.*pi*.001/6;
N_avg=(W_avg./(Dm_avg.^4))*81.487E03;

Z_num=sum(dm_6');

%selecting Dm, Nw and Z for stratiform rain using indexes determined above
Dm_avg_strat=Dm_avg(iR_strat);
avgDm=mean(Dm_avg_strat) %avg Dm for stratiform rain
std_Dm=std(Dm_avg_strat) %standard deviation of Dm for stratiform rain

Nw_strat=N_avg(iR_strat);
avgNw=mean(Nw_strat);
std_Nw=std(Nw_strat);
avg_logNw=log10(avgNw)
std_logNw=std(log10(Nw_strat))
log10(std_Nw);

Z_strat=Z_num(iR_strat);
Z=10.*(log10(Z_strat));
```

```
%determining R-Z relationship
p = polyfit(log10(Z_strat),log10(R_strat),1);
b = 1/p(1)
a = 10^(-1*p(2)*b)

%plots
figure(1)
scatter(Dm_avg_strat,log10(Nw_strat),'x');
title('Nw vs. Dm for TS Jeanne - stratiform rain');
xlabel('Dm [mm]');
ylabel('log10(Nw) [mm^-1 * m^-3]');

figure(2)
scatter(R_strat,Dm_avg_strat,'x');
title('Dm vs. rainrate for TS Jeanne - stratiform rain');
xlabel('Rainrate [mm/hr]');
ylabel('Dm [mm]');
%
figure(3)
scatter(R_strat,log10(Nw_strat),'x');
title('Nw vs. rainrate for TS Jeanne - stratiform rain');
xlabel('Rainrate [mm/hr]');
ylabel('log10(Nw) [mm^-1 * m^-3]');
%
figure(4)
hist(Dm_avg_strat,20);
title('Histogram of Dm for TS Jeanne - stratiform rain; std < 1.5');
%
figure(5)
hist(log10(Nw_strat),20);
title('Histogram of log10(Nw) for TS Jeanne - stratiform rain; std < 1.5');
%
figure(6)
scatter(Z,R_strat);
title('Reflectivity for TS Jeanne - stratiform rain');
xlabel('Z [dBZ]');
ylabel('R [mm/hr]');
plot(R_avg_calc,'-')
hold on
plot(rainrate,'r')
hold off
```